



1 **Contrasting effects of acidification and warming on dimethylsulfide** 2 **concentrations during a temperate estuarine fall bloom mesocosm** 3 **experiment**

4 Robin Bénard¹, Maurice Levasseur¹, Michael Scarratt², Sonia Michaud², Michel Starr², Alfonso Mucci³, Gustavo Ferreyra^{4,5},
5 Michel Gosselin⁴, Jean-Éric Tremblay¹, Martine Lizotte¹, Gui-Peng Yang⁶

6 ¹Département de biologie, Université Laval, 1045 avenue de la Médecine, Québec, Québec G1V 0A6, Canada

7 ²Fisheries and Oceans Canada, Maurice Lamontagne Institute, P.O. Box 1000, Mont-Joli, Québec G5H 3Z4, Canada

8 ³Department of Earth and Planetary Sciences, McGill University, 3450 University Street, Montréal, Québec H3A 2A7, Canada

9 ⁴Institut des sciences de la mer de Rimouski (ISMER), Université du Québec à Rimouski, 310 allée des Ursulines, Rimouski,
10 Québec G5L 3A1, Canada

11 ⁵Centro Austral de Investigaciones Científicas (CADIC), Consejo Nacional de Investigaciones Científicas y Técnicas,
12 Bernardo Houssay 200, 9410 Ushuaia, Tierra del Fuego, Argentina

13 ⁶Institute of Marine Chemistry, Ocean University of China, 238 Songling Road, Qingdao 266100, Shandong, China

14 *Correspondence:* Robin Bénard (robin.benard.1@ulaval.ca)

15 **Abstract.** The effects of ocean acidification and warming on the concentrations of dimethylsulfoniopropionate (DMSP) and
16 dimethylsulfide (DMS) were investigated during a mesocosm experiment in the Lower St. Lawrence Estuary (LSLE) in the
17 fall of 2014. Twelve mesocosms covering a range of p_{H_T} (pH on the total hydrogen ion concentration scale) from 8.0 to 7.2,
18 corresponding to a range of CO₂ partial pressures (pCO₂) from 440 to 2900 μatm, at two temperatures (in situ and +5 °C; 10 °C
19 and 15 °C) was monitored during 13 days. All mesocosms were characterized by the rapid development of a diatom bloom
20 dominated by *Skeletonema costatum*, followed by its decline upon the exhaustion of nitrate and silicic acid. Neither the
21 acidification nor the warming resulted in a significant impact on the abundance of bacteria over the experiment. However,
22 warming the water by 5 °C resulted in a significant increase of the average bacterial production (BP) in all 15 °C mesocosms
23 as compared to 10 °C, with no detectable effect of pCO₂ on BP. Variations in total DMSP (DMSP_t = particulate + dissolved
24 DMSP) concentrations tracked the development of the bloom although the rise in DMSP_t persisted for a few days after the
25 peaks in chlorophyll *a*. Average concentrations of DMSP_t were not affected by acidification or warming. Initially low
26 concentrations of DMS (< 1 nmol L⁻¹) increased to reach peak values ranging from 30 to 130 nmol L⁻¹ towards the end of the
27 experiment. Increasing the pCO₂ reduced the averaged DMS concentrations by 66 % and 69 % at 10 °C and 15 °C,
28 respectively, over the duration of the experiment. On the other hand, a 5 °C warming increased DMS concentrations by an
29 average of 240 % as compared to in situ temperature, resulting in a positive offset of the adverse pCO₂ impact. Significant
30 positive correlations found between bacterial production rates and concentrations of DMS throughout our experiment point
31 towards temperature-associated enhancement of bacterial DMSP metabolism as a likely driver for the mitigating effect of
32 warming on the negative impact of acidification on the net production of DMS in the LSLLE and potentially the global ocean.



33 1. Introduction

34 Dimethylsulfide (DMS) is ubiquitous in productive estuarine, coastal and marine surface waters (Barnard et al., 1982; Iverson
35 et al., 1989; Kiene and Service, 1991; Cantin et al., 1996; Kettle et al., 1999). With an estimated average 28.1 Tg of sulfur (S)
36 being transferred to the atmosphere annually (Lana et al., 2011), DMS emissions constitute the largest natural source of
37 tropospheric S (Lovelock et al., 1972; Andreae 1990; Bates et al., 1992). The oxidation of atmospheric DMS yields hygroscopic
38 sulfate (SO_4^{2-}) aerosols that directly scatter incoming solar radiation and act as nuclei upon which cloud droplets can condense
39 and grow, thereby potentially impacting cloud albedo and the radiative properties of the atmosphere (Charlson et al., 1987;
40 Andreae and Crutzen 1997; Liss and Lovelock, 2007; Woodhouse et al., 2013). The scale of the impact of biogenic SO_4^{2-}
41 particles on global climate, however, remains uncertain (Carslaw et al., 2010; Quinn and Bates, 2011, Quinn et al., 2017). The
42 strength of DMS emissions depends on wind- and temperature-driven transfer processes (Nightingale et al., 2000) but mostly
43 on its net production in the surface mixed layer of the ocean (Malin and Kirst, 1997). Net changes in the aqueous DMS
44 inventory are largely governed by microbial food webs (see reviews by Simó, 2001; Stefels et al., 2007) whose productivity is
45 potentially sensitive to modifications in the habitats that sustain them. Given the complexity of the biological cycling of DMS,
46 understanding how climate change related stressors could impact the production of this climate-active gas is a worthy but
47 formidable challenge.

48 DMS stems, for the most part, from the enzymatic breakdown of dimethylsulfoniopropionate (DMSP) (Cantoni and Anderson,
49 1956), a metabolite produced by several groups of phytoplankton, with an extensive range in intracellular quotas between taxa
50 (Keller et al., 1989; Stefels et al., 2007). Several species of the classes Haptophyceae and Dinophyceae are amongst the most
51 prolific DMSP producers, but certain members of Bacillariophyceae (diatoms) and Chrysophyceae can also produce significant
52 amounts of DMSP (Stefels et al., 2007). The biosynthesis of DMSP is highly constrained by abiotic factors and its up- or
53 down-regulation may allow cells to cope with environmental shifts in temperature, salinity, nutrients and light intensity (Kirst
54 et al., 1991; Karsten et al., 1996; Sunda et al., 2002), while its de novo synthesis and exudation may also serve as a sink for
55 excess carbon (C) and sulfur (S) under unfavourable growth conditions (Stefels, 2000). Beyond active exudation in healthy
56 cells (Laroche et al., 1999), cellular or particulate DMSP (DMSP_p) can be transferred to the water column as dissolved DMSP
57 (DMSP_d) through viral lysis (Hill et al., 1998; Malin et al., 1998), autolysis (Nguyen et al., 1988; Stefels and Van Boeckel,
58 1993), and grazing by micro-, meso- and macrozooplankton (Dacey and Wakeham, 1986; Wolfe and Steinke, 1996). The
59 turnover rate of DMSP_d in the water column is generally very rapid (a few hours to days) as this compound represents sources
60 of C and reduced S for the growth of microbial organisms (Kiene and Linn, 2000). Heterotrophic bacteria mediate most of the
61 turnover of S- DMSP_d through pathways that constrain the overall production of DMS: (1) enzymatic cleavage of DMSP_d that
62 yields DMS; (2) demethylation/ demethiolation of DMSP_d that yields methanethiol (MeSH); (3) production of dissolved non-
63 volatile S compounds, including SO_4^{2-} , following oxidation of DMSP_d ; (4) intracellular accumulation of DMSP_d with no
64 further metabolization (Kiene et al., 1999, 2000; Kiene and Linn, 2000; Yoch, 2002). A compilation of ^{35}S - DMSP_d tracer
65 studies conducted with natural microbial populations shows that microbial DMS yields rarely exceed 40% of consumed



66 DMSP_d in surface coastal and oceanic waters (see review table in Lizotte et al., 2017). Another potential fate of DMSP_d is its
67 uptake by non-DMSP producing eukaryotic phytoplankton such as certain diatoms (Vila-Costa et al., 2006b; Ruiz-González
68 et al., 2012) and cyanobacteria such as *Synechococcus* and *Prochlorococcus* (Malmstrom et al., 2005; Vila-Costa et al., 2006b),
69 but the overall turnover of DMSP_d seems to be dominated by heterotrophic organisms.

70 Whereas the role of bacteria in the production of DMS via DMSP_d is well recognized, an increasing number of studies have
71 shown that the phytoplankton-mediated enzymatic conversion of total DMSP (DMSP_t) into DMS can also be significant when
72 communities are dominated by DMSP-lyase producing phytoplankton groups such as Dinophyceae and Haptophyceae (Niki
73 et al., 2000; Steinke et al., 2002; Stefels et al., 2007; Lizotte et al., 2012), particularly under high doses of solar radiation (Toole
74 and Siegel, 2004; Toole et al., 2006, 2008; Vallina et al., 2008). Removal processes of DMS from surface waters include
75 photo-oxidation, bacterial degradation and efflux across the air-sea interface, the individual intensity of which depends on
76 several factors such as light intensity, wind velocity, the depth of the surface mixed layer and the gross production of DMS
77 (Brimblecombe and Shooter, 1986; Simó and Pedros-Alió, 1999; Nightingale et al., 2000; Hatton et al., 2004; Simó, 2004).
78 Overall, production and turnover of DMS and its precursor DMSP are unequivocally linked with microbial activity, both
79 autotrophic and heterotrophic. The associated biological processes and interactions amongst these microorganisms have been
80 shown to be sensitive to fluctuations in abiotic factors and may thus be further modulated by multiple drivers of climate change.
81 Since the pre-industrial era, atmospheric CO₂ concentrations have risen from 280 ppm, and, according to the business-as-usual
82 scenario RCP 8.5 and global ocean circulation models, are expected to reach 850–1370 ppm by 2100 (IPCC, 2013). The oceans
83 have already absorbed about 28 % of the anthropogenic CO₂ emitted to the atmosphere (Le Quéré et al., 2015), leading to a
84 pH decrease of 0.11 units in surface waters (Gattuso et al., 2015), a phenomenon called ocean acidification (OA). An additional
85 decrease of pH by 0.3–0.4 units is expected by the end of this century, and could reach 0.8 units by 2300 (Caldeira and Wickett,
86 2005; Doney et al., 2009; Feely et al., 2009). In addition to the oceanic sink, a similar fraction of anthropogenic CO₂ emissions
87 has been captured by terrestrial vegetation. while the anthropogenic CO₂ remaining (45% of total emissions) in the atmosphere
88 (Le Quéré et al., 2013) has led to an estimated increased greenhouse effect of 0.3–0.6 W m⁻² globally over the past 135 years
89 (Roemmich et al., 2015). Ninety percent of this excess heat has been absorbed by the ocean, increasing sea surface temperatures
90 (SST) ~0.1 °C per decade since 1951 and could increase SST by 3–5 °C before 2100 (IPCC, 2013). Leading experts in the
91 field of global change have called upon the scientific community to address critical knowledge gaps, among which, a top
92 priority remains the assessment of the impact of multiple environmental stressors on marine microorganisms (Riebesell and
93 Gattuso, 2015).

94 The sensitivity of natural planktonic assemblages to OA, along with their production of DMSP and DMS, has been investigated
95 in several experimental studies (see review table in Hussherr et al., 2017). The majority of these experiments have shown a
96 decrease in both DMSP and DMS concentrations with increasing pCO₂ (Hopkins et al., 2010; Avgoustidi et al., 2012; Park et
97 al., 2014; Webb et al., 2015). The decrease in DMSP production has largely been attributed to the deleterious impact of
98 decreasing pH on the coccolithophore *Emiliana huxleyi*, the dominant DMSP producer in several of these studies.
99 Nevertheless, OA does not always result in a concomitant decrease in DMSP and DMS production. For example, the pCO₂-



100 induced decrease in DMS reported by Archer et al. (2013) in Arctic waters was accompanied by an increase in DMSP
101 concentrations, indicating that DMS production is at least partly dependent on the turnover of DMSP, rather than on the DMSP
102 pool. A modeling study showed that the specific implementation of the negative effect of OA on DMS net production in a
103 coupled ocean-atmosphere model reduces global DMS production by $18 \pm 3\%$, resulting in an additional warming of 0.23–
104 0.48 K by 2100 under the A1B scenario (Six et al., 2013). Schwinger et al. (2017) further showed that the OA-induced
105 decreases in oceanic DMS emissions could result in a transient global warming of 0.30 K, mostly resulting from a reduction
106 of cloud albedo. These first attempts to model the potential effect of OA on climate through its impact on DMS oceanic
107 production show that OA may significantly affect climate by reducing marine emissions of DMS but also highlight the
108 importance of carefully assessing the robustness of the DMS-OA negative relationship. This is particularly relevant considering
109 that some experiments reveal a neutral or positive effect of increasing $p\text{CO}_2$ on DMS net production (Vogt et al., 2008; Kim
110 et al., 2010; Hopkins and Archer, 2014). Regional or seasonal differences in phytoplankton taxonomy, microzooplankton
111 grazing, and bacterial activity have been proposed as key drivers of the discrepancies between these experimental results.

112 Whereas studies of the impact of OA on DMS cycling have gained momentum, the importance of assessing how combined
113 drivers of change may impact the structure and the functioning of ocean ecosystems, using multifactorial approaches, is now
114 increasingly recognized (Boyd et al., 2015; 2018; Riebesell and Gattuso, 2015; Gunderson et al., 2016). Thus far, only two
115 mesocosm studies assessed the combined effect of OA and warming on DMS dynamics by natural plankton assemblages. The
116 two studies, both conducted with coastal waters, led to contrasting results. The first study showed an 80 % increase in DMS
117 concentrations under high $p\text{CO}_2$ conditions (900 ppm vs. 400 ppm), and a reduction by 20 % of this stimulating effect when
118 the increase in $p\text{CO}_2$ was accompanied by a 3 °C warming (Kim et al., 2010). However, the absence of a specific stand-alone
119 warming treatment did not allow the authors to assess the sole impact of temperature on DMS net production. The second
120 study showed decreasing DMS concentrations under both acidification and greenhouse conditions, with the lowest DMS
121 concentrations measured under combined acidification and warming treatments (Park et al., 2014). The authors attributed these
122 contrasting responses to differences in the phytoplankton assemblages, DMSP-related algal physiological characteristics, and
123 microzooplankton grazing. Nevertheless, questions remain as to the combined effect of $p\text{CO}_2$ and warming on DMS net
124 production since the temperature treatments were not conducted over the full range of $p\text{CO}_2$ tested (Kim et al., 2010; Park et
125 al., 2014).

126 The combined influence of acidification and warming on the dynamics of the St. Lawrence Estuary phytoplankton fall bloom
127 was investigated during a full factorial mesocosm experiment (Bénard et al., 2018). During this experiment, a bloom of
128 *Skeletonema costatum* developed in all mesocosms, independently of the $p\text{CO}_2$ gradient (from 440 to 2900 μatm) and
129 temperatures tested (10 and 15 °C). The increase in $p\text{CO}_2$ had no influence on the bloom but warming accelerated the growth
130 rate of the diatoms and hastened the decline of the bloom (Bénard et al., 2018). Here, we report on the impacts of acidification
131 and warming on DMSP and DMS concentrations with a focus on the dynamics of heterotrophic bacteria, a component of the
132 marine food web known to affect the turnover of DMSP and DMS.



133 2. Material and methods

134 2.1 Mesocosm setup

135 The mesocosm experimental setup is described in detail in B nard et al. (2018). Briefly, mesocosm experiments were
136 conducted at the ISMER marine research station of Rimouski (Qu bec, Canada) in the fall of 2014. The twelve 2600 L
137 cylindrical (2.67 m \times 1.4 m), conical bottom, mesocosms were housed in two temperature-controlled, full-size shipping
138 containers each containing six mesocosms (Aquabiotech Inc., Qu bec, Canada). Each mesocosm are mixed by a propeller
139 secured near the top of each enclosure to ensure homogeneous vertical mixing of the water column. The mesocosms are sealed
140 by a Plexiglas cover transmitting 50–85 % of solar UVB (280–315 nm), 85–90 % of UVA (315–400 nm), and 90 % of
141 photosynthetically active radiation (PAR; 400–700 nm) of the natural incident light. Independent temperature probes (AQBT-
142 Temperature sensor, accuracy ± 0.2 $^{\circ}\text{C}$) were installed in each mesocosm, recording temperature every 15 minutes and either
143 triggering a resistance heater (Process Technology TTA1.8215) or a glycol refrigeration system activated by an automated
144 pump. The pH of the mesocosms was measured every 15 minutes by Hach[®] PD1P1 probes (± 0.02 pH units) linked to Hach[®]
145 SC200 controllers. To maintain pH, two reservoirs of artificial seawater were equilibrated with pure CO₂ before the start of
146 the experiment and positive deviations from the target pH values in each mesocosm activated peristaltic pumps that injected
147 the CO₂ supersaturated seawater into the mesocosm water. This control system was able to maintain the pH in the mesocosms
148 within ± 0.02 pH units of the targeted values during the initial bloom development by lowering the pH, but it could not increase
149 the pH during the declining phase of the bloom.

150 2.2 Experimental approach

151 Prior to the onset of the experiment, all the mesocosms were meticulously washed with diluted VirkonTM, an anti-viral and
152 anti-bacterial solution, according to the manufacturer’s instructions (Antec International Limited), and thoroughly rinsed. The
153 experimental approach is also detailed in B nard et al. (2018). To fill the mesocosms, water from ~ 5 m depth was collected
154 near the Rimouski harbour (48 $^{\circ}$ 28' 39.9" N, 68 $^{\circ}$ 31' 03.0" W) on the 27th of September 2014 (day -5). Initial conditions were:
155 practical salinity (S_p) = 26.52, temperature = 10 $^{\circ}\text{C}$, nitrate (NO_3^-) = 12.8 ± 0.6 $\mu\text{mol L}^{-1}$, silicic acid
156 ($\text{Si}(\text{OH})_4$) = 16 ± 2 $\mu\text{mol L}^{-1}$, and soluble reactive phosphate (SRP) = 1.4 ± 0.3 $\mu\text{mol L}^{-1}$. Following its collection, the water
157 was screened through a 250 μm mesh while the mesocosms were simultaneously gravity-filled by a custom made “octopus”
158 tubing system. The initial in situ temperature of 10 $^{\circ}\text{C}$ was maintained in all mesocosms for the first 24 h (day -4). On day -3,
159 the six mesocosms in one of the containers were gradually heated to 15 $^{\circ}\text{C}$ while the mesocosms in the other container were
160 maintained at 10 $^{\circ}\text{C}$. No manipulations were carried on day -2 to avoid excessive stress, and acidification was carried out on
161 day -1. The mesocosms were initially set to cover a gradient of pH_T (total proton concentration scale) of ~ 8.0 to 7.2
162 corresponding to a range of pCO₂ from 440 to 2900 μatm . Two mesocosms, one in each container (at each temperature), were
163 not pH-controlled to assess the effect of freely fluctuating pH condition. These two mesocosms were called drifters since the
164 in-situ pH was allowed to drift over time throughout the bloom development. To achieve the initially targeted pH_T, CO₂-



165 saturated artificial seawater was added to mesocosms M1, M3, M5, M7, M8, M10 (pH_T 7.2–7.6) while mesocosms M2, M4,
166 M6, M9, M11, M12 (pH_T 7.8–8.0 and the drifters) were openly mixed to allow CO₂ degassing. Then, the automatic system
167 controlling the occasional addition of CO₂-saturated artificial seawater maintained the pH equal or below the targeted pH, except
168 for the drifters.

169 2.3 Seawater analysis

170 Daily sampling of the mesocosms was carried out between 05:00 and 08:00 every day (EDT) as described in Bénard et al.
171 (2018). Samples for carbonate chemistry, nutrients, DMSP and DMS were collected directly from the mesocosms prior to
172 filling of 20 L carboys from which seawater for the determination of chlorophyll *a* (Chl *a*), bacterial abundance, and bacterial
173 production (BP) was subsampled. Samples were collected directly from the mesocosms and the artificial seawater tank on days
174 -3, 3 and 13 for practical salinity determinations. The samples were collected in 250 mL plastic bottles and stored in the dark
175 until analysis was carried out on a Guildline Autosol 8400B salinometer in the months following the experiment.

176 2.3.1 Carbonate chemistry and nutrients

177 Analytical methods used to determine the carbonate parameters are described in detail in Bénard et al. (2018). Briefly, pH was
178 determined every day by transferring samples from the mesocosms to 125 mL plastic bottles without headspace. The samples
179 were analyzed within hours of collection on a Hewlett-Packard UV-Visible diode array spectrophotometer (HP-8453A) and a
180 5 cm quartz cell using phenol red (PR; Robert-Baldo et al., 1985) and *m*-cresol purple (mCP; Clayton and Byrne, 1993) as
181 indicators after equilibration to 25.0 ± 0.1 °C in a thermostated bath. The pH on the total proton scale (pH_T) was calculated
182 according to Byrne (1987), with the salinity of the sample and the HSO₄⁻ association constants given by Dickson (1990). The
183 reproducibility of pH measurements, based on replicate measurements of the same samples and values derived from both
184 indicators, was on the order of 0.003. Total alkalinity (TA) samples were collected every 3–4 days in 250 mL glass bottles to
185 which a few crystals of HgCl₂ were added before sealing with ground glass stoppers and Apiezon[®] Type-M high-vacuum
186 grease. The TA determinations were carried out within one day of sampling by open-cell automated potentiometric titration
187 (Titrilab 865, Radiometer[®]) with a pH combination electrode (pHC2001, Red Rod[®]) and a dilute (0.025 M) HCl titrant solution
188 calibrated against Certified Reference Materials (CRM Batch#94, provided by A. G. Dickson, Scripps Institute of
189 Oceanography, La Jolla, USA). The average relative error, calculated from the average relative standard deviation on replicate
190 standards and sample analyses, was < 0.15 %. The computed pH_T at 25 °C, measured TA, silicic acid and SRP concentrations
191 were used to calculate the in situ pH_T, pCO₂ and saturation state of the water in each mesocosm using CO₂SYS (Pierrot et al.,
192 2006) and the carbonic acid dissociation constants of Cai and Wang (1998).

193 The samples for the determination of NO₃⁻, Si(OH)₄, and SRP were filtered through Whatman GF/F filters, collected in acid
194 washed polyethylene tubes and stored at -20 °C. Analysis was carried out using a Bran and Luebbe Autoanalyzer III using the
195 colorimetric methods of Hansen and Koroleff (2007). The analytical detection limit was 0.03 μmol L⁻¹ for NO₃⁻ plus nitrite
196 (NO₂⁻), 0.02 μmol L⁻¹ for NO₂⁻, 0.1 μmol L⁻¹ for Si(OH)₄, and 0.05 μmol L⁻¹ for SRP.



197 2.3.2 Biological variables

198 Chl *a* determination methods are presented in Bénard et al. (2018). Succinctly, duplicate 100 mL samples were filtered onto
199 Whatman GF/F filters. The filters were soaked in a 90 % acetone solution at 4 °C in the dark for 24 h, the solution was then
200 analyzed by a 10-AU Turner Designs fluorometer (acidification method: Parsons et al., 1984). The analytical detection limit
201 for Chl *a* was 0.05 µg L⁻¹.

202 Samples for the determination of free-living heterotrophic bacteria were kept in sterile cryogenic polypropylene vials and fixed
203 with glutaraldehyde Grade I (final concentration = 0.5 %, Sigma Aldrich; Marie et al., 2005). Duplicate samples were placed
204 at 4 °C in the dark for 30 min, then frozen at -80 °C until analysis by a FACS Calibur flow cytometer (Becton Dickinson)
205 equipped with a 488 nm argon laser. Before enumeration, the samples were stained with SYBR Green I (0.1 % final
206 concentration, Invitrogen Inc.) to which 600 µl of a Tris-EDTA 10 × buffer of pH 8 were added (Laboratoire MAT; Belzile et
207 al., 2008). Fluoresbrite beads (diameter 1 µm, Polysciences) were also added to the sample as an internal standard. The green
208 fluorescence of SYBR Green I was measured at 525 ± 5 nm. Bacterial abundance was determined as the sum of low and high
209 nucleic (LNA and HNA) counts (Annane et al., 2015).

210 Bacterial production was estimated in each mesocosm on days 0, 2, 4, 6, 8, 10, 11 and 13 by measuring incorporation rates of
211 tritiated thymidine (³H-TdR), using an incubation and filtration protocol based on Fuhrman and Azam (1980, 1982). Twenty
212 mL water subsamples were transferred from glass Erlenmeyers to five sterile glass vials; three as “measured” values and two
213 as blanks. In all blank vials, 0.2 mL of formaldehyde 37 % were added, immediately after the sampling to stop all biological
214 activities. Then, 1 mL of ³H-TdR solution (4 µmol L⁻¹), prepared from commercial solution (63 Curie mmol⁻¹; 1 mCurie mL⁻¹,
215 10 µmol L⁻¹ ³H-TdR, MP Biomedicals), was added in all vials. Samples were incubated 2.5 h at experimental temperatures
216 (10 or 15 °C), and then 0.2 mL of formaldehyde 37 % were immediately added in the three “measure” vials. Bacteria were
217 then collected by filtration (diameter 25 mm; 0.2 µm porosity) and filters were treated according to Fuhrman and Azam (1980,
218 1982). ³H-TdR incorporation was measured using a scintillation counter (Beckman LS5801) and results were expressed in
219 dpm. Blank values were subtracted to “measured” values to remove background radioactivity. ³H-TdR incorporation rates
220 were converted in mole of ³H-TdR incorporated per unit of volume and time, before converting to rate of carbon production
221 using the carbon conversion factor of Bell (1993).

222 2.3.3 DMSP and DMS concentrations

223 For the quantification of DMSP_t, duplicate 3.5 mL samples of seawater were collected into 5 mL polyethylene tubes. Samples
224 were preserved by adding 50 µL of a 50 % sulfuric acid solution (H₂SO₄) to the tubes before storage at 4 °C in the dark until
225 analysis in the following months. Samples for the quantification of DMSP_d were taken daily, but a technical problem during
226 storage and transport of the samples led to a loss of all samples. The DMSP samples were injected into a purge and trap (PnT)
227 system before being completely flushed using 1–5 mL Milli-Q™ water into the helium purged chamber heated to 70 °C. DMSP
228 concentrations were determined by a mole to mole conversion to DMS following hydrolysis with a 5 M NaOH solution injected



229 in the chamber prior to the sample, and trapping the gas sample in a loop immersed in liquid nitrogen. The loop was then
230 heated in a water bath to release the trapped sample and analyzed using a Varian 3800 Gas Chromatograph equipped with a
231 pulsed flame photometric detector (PFPD, Varian 3800) and a detection limit of 0.9 nmol L^{-1} (Scarratt et al., 2000; Lizotte et
232 al., 2012).

233 Samples for the quantification of DMS were directly collected from the mesocosms into 20 mL glass vials with a butyl septa
234 and aluminum crimp. The samples were kept in the dark at $4 \text{ }^{\circ}\text{C}$ until analysis was carried out within hours of collection using
235 the PnT system described above.

236 2.4 Statistical analyses

237 The statistical analyses were performed using the nlme package in R (R Core Team, 2016). The data were analyzed using a
238 general least squares (gls) approach to test the linear effects of the two treatments (temperature, pCO_2), and their interaction
239 on the variables (Paul et al., 2016; Hussherr et al., 2017; Bénard et al., 2018). The analyses were conducted on the averages of
240 the measured parameters over the whole duration of the experiment, and separate regressions for pCO_2 were performed for
241 each temperature when the latter had a significant effect. The residuals were checked for normality using a Shapiro-Wilk test
242 ($p > 0.05$) and data were transformed (square root or natural logarithm) if necessary. In addition, squared Pearson's correlation
243 coefficients (r^2) with a significance level of 0.05 were used to evaluate correlations between key variables.

244 3. Results

245 3.1 Physical and chemical conditions during the experiments

246 The S_p was 26.52 ± 0.03 on day -4 in all mesocosms and remained constant throughout the experiment, averaging 26.54 ± 0.02
247 on day 13 (Bénard et al., 2018). The temperature of the mesocosms in each container remained within $\pm 0.1 \text{ }^{\circ}\text{C}$ of the target
248 temperature throughout the experiment and averaged $10.04 \pm 0.02 \text{ }^{\circ}\text{C}$ for mesocosms M1 through M6, and $15.0 \pm 0.1 \text{ }^{\circ}\text{C}$ for
249 mesocosms M7 through M12 (Fig. 1a). The pH_T remained relatively stable throughout the experiment in the pH-controlled
250 treatments, but decreased slightly as the experiment progressed, deviating by an average of -0.14 ± 0.07 units relative to the
251 target pH_T on the last day (Fig. 1b). The pH variations corresponded to changes in pCO_2 from an average of $1340 \pm 150 \text{ } \mu\text{atm}$
252 on day -3, and ranged from 564 to 2902 μatm at $10 \text{ }^{\circ}\text{C}$ and from 363 to 2884 μatm at $15 \text{ }^{\circ}\text{C}$ on day 0 following the acidification
253 (Fig. 1c). The in situ pH_T in the drifters (M6 and M11) increased from 7.896 and 7.862 on day 0, at $10 \text{ }^{\circ}\text{C}$ and $15 \text{ }^{\circ}\text{C}$
254 respectively, to 8.307 and 8.554 on day 13, reflecting the balance between CO_2 uptake and metabolic CO_2 production over the
255 duration of the experiment. On the last day, pCO_2 in all mesocosms ranged from 186 to 3695 μatm at $10 \text{ }^{\circ}\text{C}$ and from 90 to
256 3480 μatm at $15 \text{ }^{\circ}\text{C}$.

257 Nitrate (NO_3^-) and silicic acid (Si(OH)_4) concentrations averaged $9.1 \pm 0.5 \text{ } \mu\text{mol L}^{-1}$ and $13.4 \pm 0.3 \text{ } \mu\text{mol L}^{-1}$ on day 0,
258 respectively (Bénard et al., 2018). The two nutrients displayed a similar temporal depletion pattern following the development
259 of the phytoplankton bloom. NO_3^- concentrations reached undetectable levels ($< 0.03 \text{ } \mu\text{mol L}^{-1}$) in all mesocosms by day 5.



260 Likewise, $\text{Si}(\text{OH})_4$ fell below the detection limit ($< 0.1 \mu\text{mol L}^{-1}$) between day 1 and 5 in all mesocosms except for those whose
261 pH_T was set at 7.2 and 7.6 at 10°C (M5 and M3) and in which $\text{Si}(\text{OH})_4$ depletion occurred on day 9.

262 3.2 Phytoplankton, bacterial abundance and production

263 Chl *a* concentrations were below $1 \mu\text{g L}^{-1}$ following the filling of the mesocosms (day -4), and had already increased to an
264 average of $5.9 \pm 0.6 \mu\text{g L}^{-1}$ on day 0 (Fig. 2a). At 10°C , Chl *a* quickly increased to reach maximum concentrations around
265 $27 \pm 2 \mu\text{g L}^{-1}$ on day 3 ± 2 , and decreased progressively until the end of the experiment. Increasing the temperature by 5°C
266 resulted in a more rapid development of the bloom and a speedier decrease of Chl *a* concentrations during the declining phase
267 of the bloom. The maximum Chl *a* concentration reached at the peak of the bloom was, however, not significantly affected by
268 the difference in temperature. We found no significant effect of the pCO_2 gradient on the mean Chl *a* concentrations measured
269 over the days 0–13, nor during the development phase and the declining phase of the bloom as described in B nard et al. (2018)
270 (Fig. 2a–b; Table 1).

271 The free-living bacterial abundance was $\sim 1.2 \times 10^9 \text{ cells L}^{-1}$ on day -4, and increased rapidly to reach $3.1 \pm 0.6 \times 10^9 \text{ cells L}^{-1}$
272 on day 0 (Fig. 2c). This initial increase in abundance probably resulted from the release of dissolved organic matter (DOM)
273 during pumping of the seawater and filling of the mesocosms. The subsequent decrease in bacterial abundance during the
274 development phase of the bloom suggests that the initial pool of DOM was fully utilized and that freshly released DOM was
275 scarce. As expected, bacterial abundance increased during the declining phase of the bloom at 10°C . Under warmer conditions,
276 bacterial abundance decreased earlier during the initial bloom development than what was observed at 10°C , but was also
277 marked by an earlier peak during the decline of the bloom, then was followed by a second, more variable peak in abundance.
278 These daily variations in abundances probably reflect changes in the balance between bacterial growth and loss by grazing.
279 When averaged over the experiment, we observed no effect of the treatments on the mean bacterial abundance (Fig. 2c–d;
280 Table 1). At 10°C , bacterial production was low at the beginning of the experiment and increased gradually during the
281 development and declining phases of the bloom to reach peak values of $9.3 \pm 0.9 \mu\text{g C L}^{-1} \text{ d}^{-1}$ (Fig. 2e). Bacterial production
282 increased faster at 15°C and reached maximal production rates of $19 \pm 1 \mu\text{g C L}^{-1} \text{ d}^{-1}$ on day 11. Results of the gls model show
283 no effect of the pCO_2 gradient on bacterial production, but a positive effect of warming was observable throughout the
284 experiment (Fig. 2f; Table 1).

285 3.3 DMSP_i and DMS

286 At in situ temperature, DMSP_i concentrations averaged $9 \pm 2 \text{ nmol L}^{-1}$ on day 0 and increased regularly in all mesocosms up
287 to day 10 before they plateaued or slightly decreased over the last 2–3 days (Fig. 3a). These results reveal that DMSP_i
288 accumulation persisted for several days after the bloom peaks, to reach a maximum value between days 8–13 of
289 $366 \pm 22 \text{ nmol L}^{-1}$. At 15°C , DMSP_i concentrations similarly increased after the maximum Chl *a* concentrations were reached,
290 but increased faster than at in situ temperature. The maximum DMSP_i concentrations were $396 \pm 19 \text{ nmol L}^{-1}$ at 15°C , a value



291 that is not statistically different from the peak values measured at 10 °C (Fig 4a; Table 2). A greater loss of DMSP took place
292 in the last days of the experiment at 15 °C. By day 13, 79 ± 3 % of the peak DMSP_t concentration was lost in the 15 °C
293 mesocosms, while 19 ± 4 % of the peak DMSP_t concentration was lost at 10 °C. When averaged over the duration of the
294 experiment, the mean DMSP_t concentrations were not significantly affected by the pCO_2 gradient, the temperatures or the
295 interaction between these two factors (Fig. 3b; Table 1).

296 Over the 13 days, the $\text{DMSP}_t:\text{Chl } a$ ratio averaged 11.4 ± 0.4 nmol ($\mu\text{g Chl } a$)⁻¹ at 10 °C and was not affected by increasing
297 pCO_2 (Fig. 5a; Table 1). Due to the aforementioned mismatch between the peaks in $\text{Chl } a$ and DMSP_t , the average
298 $\text{DMSP}_t:\text{Chl } a$ ratios were significantly higher at 15 °C, averaging 19 ± 1 nmol ($\mu\text{g Chl } a$)⁻¹ over the experiment (Fig. 5a; Table
299 1). However, we found no significant relationship between $\text{DMSP}_t:\text{Chl } a$ and the pCO_2 gradient.

300 Initial DMS concentrations were below the detection limit on day 0 (< 0.9 nmol L⁻¹) and slowly increased during the first 7
301 days, while most of the build-up took place after day 8 in all treatments (Fig. 3b). The net accumulation of DMS was faster at
302 15 °C than at 10 °C, with higher daily DMS concentrations at 15 °C compared to 10 °C from day 3 until day 13. At the end of
303 the experiment, DMS concentrations averaged 21 ± 4 nmol L⁻¹ at 10 °C and 74 ± 14 nmol L⁻¹ at 15 °C. Over the full duration
304 of the experiment, we found significant negative effects of increasing pCO_2 on mean DMS concentrations at the two
305 temperatures tested (Fig. 3c; Table 1). At 10 °C, we measured a ~67 % reduction of mean DMS concentrations from the drifter
306 relative to the most acidified treatment (~345 ppm vs ~3200 ppm), with values decreasing from 10 ± 2 nmol L⁻¹ to
307 3.2 ± 0.8 nmol L⁻¹. At 15 °C, the mean DMS concentrations decreased by roughly the same percentage (~69 %) as pCO_2
308 increased from the drifter to the most acidified treatment (~130 ppm vs ~3130 ppm). Nevertheless, the mean DMS
309 concentrations were higher at 15 °C, ranging from 34 ± 13 nmol L⁻¹ to 11 ± 3 nmol L⁻¹ (Fig. 3c; Table 1). Similarly, the peak
310 DMS concentrations decreased linearly with increasing pCO_2 at both temperatures and concentrations were always higher at
311 15 than at 10 °C for any given pCO_2 (Fig. 4b; Table 2).

312 The $\text{DMS}:\text{Chl } a$ ratios remained below 1 nmol ($\mu\text{g Chl } a$)⁻¹ during the first 8 days in all mesocosms as DMS concentrations
313 were low, but increased exponentially at 15 °C in the following days. At 10 °C, the $\text{DMS}:\text{Chl } a$ ratio averaged
314 0.43 ± 0.7 nmol ($\mu\text{g Chl } a$)⁻¹ over the 13 days and was not affected by the pCO_2 gradient. At 15 °C, the $\text{DMS}:\text{Chl } a$ ratios were
315 not significantly affected by the pCO_2 gradient, but were significantly higher in the warmer treatment (Fig. 5b; Table 1).

316 The $\text{DMS}:\text{DMSP}_t$ ratio exhibited the same general pattern as the DMS, i.e. low and stable values during the first 8 days, and
317 increasing values between days 8–13 (Fig. 3e). The natural logarithm of the $\text{DMS}:\text{DMSP}_t$ ratio was not affected by the pCO_2
318 gradient at 10 °C when averaged over the 13 days experiment, but a significant decrease of the $\text{DMS}:\text{DMSP}_t$ ratios was
319 observed with increasing pCO_2 at 15 compared to 10 °C (Fig. 3f; Table 1).



320 4. Discussion

321 4.1 General characteristics

322 As far as we know, this study is the first full factorial mesocosm experiment where all pCO₂ treatments (pH_T from 8.0 to 7.2)
323 were replicated at two different temperatures (in situ and +5 °C), to assess the impact of ocean acidification and warming on
324 the dynamics of DMSP and DMS concentrations during a phytoplankton bloom. A diatom bloom dominated by *Skeletonema*
325 *costatum* developed in all mesocosms, regardless of the treatments. This chain-forming centric diatom is a cosmopolitan
326 species in coastal and estuarine systems and a frequent bloomer in the Lower St. Lawrence Estuary (LSLE) (Kim et al., 2004;
327 Starr et al., 2004; Annane et al., 2015). The 13 days where treatments were applied allowed us to capture the development and
328 declining phases of the bloom. The impacts of the treatments on the dynamics of the bloom during these two phases are
329 described in greater details in Bénard et al. (2018). Briefly, the acidification had no detectable effect on the development rate
330 of the diatom bloom and on the maximum Chl *a* concentrations reached. However, increasing the water temperature by 5 °C
331 increased the growth rate of the diatoms, shortening the development phase of the bloom, from 4–7 days at 10 °C to 1–4 days
332 at 15 °C. However, these changes in the bloom timing did not alter the overall primary production throughout the experiment.
333 Hereafter, we discuss how increasing pCO₂ (lowering the pH) affected DMSP and DMS concentrations and how a 5 °C
334 increase in temperature altered the impacts of the pCO₂ gradient during the experiment.

335 4.2. DMSP dynamics

336 The buildup of the phytoplankton biomass during the bloom development was coupled with a rapid increase in DMSP_t
337 concentrations (Fig. 3a). Assuming that *S. costatum* was responsible for most of the DMSP production, our results indicate a
338 low sensitivity of the DMSP synthesis pathway to acidification in this species. The net accumulation of DMSP_t persisted
339 several days after the peaks in Chl *a*, indicating a decoupling between DMSP synthesis, algal growth and nitrogen metabolism
340 (Bénard et al., 2018).

341 4.2.1 Effects of acidification on DMSP

342 At in situ temperature, the averaged DMSP_t concentrations were not affected by the increase in pCO₂ (Fig. 3b; Table 1). The
343 lack of significant changes in the DMSP_t:Chl *a* ratio as a function of the pCO₂ gradient also supports this conclusion (Fig. 5a;
344 Table 1). This result is consistent with those of previous studies that showed a relatively weak effect of an increase in pCO₂
345 on DMSP concentrations (Vogt et al., 2008; Lee et al., 2009; Avgoustidi et al., 2012; Archer et al., 2013; Webb et al., 2015).
346 Furthermore, much like the patterns observed at 10 °C, there was no relationship between the concentrations of DMSP_t and
347 the pCO₂ gradient observable at 15 °C (Table 1).



348 4.2.2 Effects of warming on DMSP

349 In contrast to the absence of effects of acidification on DMSP, warming has been previously shown to affect DMSP
350 concentrations in nature. Results from shipboard incubation experiments conducted in the North Atlantic have revealed an
351 increase in particulate DMSP (DMSP_p) concentrations due to a 4 °C warming (Lee et al., 2009). During this last study, the
352 higher DMSP_p concentrations were attributed to a temperature-induced shift in community structure toward species with higher
353 cellular DMSP content. During our study, the pCO₂ and temperature treatments did not alter the structure of the community
354 (Bénard et al., 2018). Most of the DMSP synthesis was likely linked to the numerically dominant diatoms, as all other algal
355 groups identified contributed to less than 10 % of the total algal abundance (see Fig. 6 in Bénard et al., 2018). Our results thus
356 suggest that DMSP synthesis by *S. costatum* during the nitrate-replete growth phase was not significantly affected by warming.
357 Rather, it is the accelerated growth rate of *S. costatum* that promoted the concurrent accumulation of biomass and DMSP_p,
358 while the higher DMSP_p:Chl *a* ratio observable at 15 °C may be explained by the faster degradation of cells under warming.
359 Several empty frustules were found during the last days of the experiment at 15 °C, suggesting a loss of integrity of the cells
360 and potential increase of the release of intracellular dissolved organic matter, including DMSP. The increase in the abundance
361 of bacteria and in bacterial production (Fig. 2c, e) during that period also suggest that more dissolved organic matter was
362 produced during the decline of the bloom, as previously reported (Engel et al., 2004a, 2004b). During our experiment,
363 transparent exopolymer particles (TEP) concentrations increased during this period (Gaaloul, 2017), adding to the evidence
364 for heightened DOM production by the decaying bloom, with a potential increase in DMSP metabolization by heterotrophic
365 bacteria under warming.

366 4.3 DMS dynamics

367 DMS concentrations remained very low during the development phase of the bloom (day 8) and increased in the latter days of
368 the experiment. Most of the DMS accumulation in the mesocosms took place between days 8–13 and likely originated from
369 DMSP that may have been released during cell lysis (Kwint and Kramer, 1995), or upon zooplankton grazing (Cantin et al.,
370 1996). Unbalanced growth and photosynthesis of algal cells under nitrogen deficiency during that period may also be
371 responsible for a greater production and active exudation of DMSP (Stefels et al., 2000; Kettles et al., 2014).

372 4.3.1 Effects of acidification on DMS

373 At in-situ temperature, we observed a significant linear decrease in DMS concentrations (both averaged over the full duration
374 of the experiment and peak concentrations) with increasing pCO₂ (Figs. 3c, 4b; Tables 1 and 2). Several earlier mesocosm
375 experiments have shown similar decreasing trends of DMS concentrations with increasing pCO₂ (Hopkins et al., 2010; Archer
376 et al., 2013; Park et al., 2014; Webb et al., 2015, 2016). In these studies, the pCO₂-induced decreases in DMS were generally
377 attributed to changes in the microbial community speciation and structure, or to microzooplankton grazing, although decreases
378 in bacterial DMSP-to-DMS conversion or increases in DMS consumption have also been suggested (Archer et al., 2013;



379 Hussherr et al., 2017). During our study, the decrease in DMS concentrations with increasing pCO₂ cannot be directly attributed
380 to a decrease in DMSP_i since this pool was not affected by the pCO₂ gradient (Figs. 3b, 4a; Tables 1 and 2). In Park et al.
381 (2014), the increase in pCO₂ led to the reduction in the abundance of *Alexandrium* spp., an active DMSP and DMSP-Lyase
382 (DLA) producer, and a concomitant reduction of the associated microzooplankton grazing. As *Alexandrium* spp. was less
383 numerous, the associated attenuation of microzooplankton grazing resulted in a reduction of the mixing of DMSP and DLA,
384 leading to lesser DMSP-to-DMS conversion. Given the strong contribution of *S. costatum* to the bloom, a species with no
385 reported DLA, it can be assumed that most, if not all, of the DMS produced was driven by bacterial processes following DMSP
386 release by the diatoms. Thus, the decrease in DMS concentrations in our study could have been the result of altered bacterial
387 mediation; either through reduced bacterial production of DMS or heightened bacterial consumption of DMS. Whereas a
388 reduction in bacterial uptake of DMSP is unlikely, given that the bacterial abundance and production were unaffected by the
389 pCO₂ gradient (Table 1), the observed decrease in DMS concentrations could imply that at higher pCO₂ the bacterial yields of
390 DMS are abated. The relative proportion of DMSP consumed by bacteria and further cleaved into DMS is closely tied to
391 bacterial demand in carbon and sulfur as well as to the availability of DMSP relative to other sources of reduced sulfur in the
392 environment (Levasseur et al., 1996; Kiene et al., 2000; Pinhassi et al., 2005). The absence of a significant pCO₂ effect on the
393 concentrations of DMSP during this study may be interpreted as a pCO₂-related alteration of the microbially-mediated fate of
394 consumed DMSP. Unfortunately, in the absence of detailed ³⁵S-DMSP_d bioassays, it is impossible to confirm the outcome of
395 the DMSP metabolic pathways including the DMSP-to-DMS conversion efficiency in relation to the pCO₂ gradient. A few
396 studies (Grossart et al., 2006; Engel et al., 2014; Webb et al., 2015;) have reported enhanced bacterial abundance and
397 production at high pCO₂, especially for attached bacteria as opposed to free-living (Grossart et al., 2006). However, regardless
398 of the temperature treatment, neither the abundance nor the activity of bacteria seemed to be significantly impacted by pCO₂
399 in this study. A pCO₂-induced increase in bacterial DMS turnover could also explain the decrease in DMS concentrations, but
400 several studies suggest that bacterial DMS consumption in natural systems is often tightly coupled to DMS production itself
401 (Simó, 2001, 2004). Furthermore, while one laboratory study reported that non-limiting supplies of DMS may be used as a
402 substrate by several members of Bacteroidetes (Green et al., 2011), another study showed that only a subset of the natural
403 microbial population may turnover naturally-occurring levels of DMS (Vila-Costa et al., 2006b). Nevertheless, the sensitivity
404 of these DMS-consuming bacteria to decreasing pH remains unknown. Likewise, whereas we cannot exclude a potential impact
405 of pCO₂ on DMS turnover via bacterioplankton, it is plausible that the pCO₂ gradient may have affected a widespread
406 physiological pathway among bacteria, specifically, the metabolic breakdown of DMSP.

407 4.3.2 Effects of warming on DMS

408 A warming by 5 °C increased DMS concentrations at all pCO₂ tested, resulting in an offset of the negative pCO₂ impact when
409 compared to the in situ temperature. This result differs from the observation of Kim et al. (2010) and Park et al. (2014) in two
410 ways. First, our results show an increase in DMS concentrations in the warmer treatment while the two previous studies
411 reported a decrease. Second, our results confirm that a temperature effect may be measured over a large range of pCO₂. It is



412 noteworthy that the increase in DMS concentrations at the two temperatures tested varied from 110 % at pH 8.0 up to 370 %
413 at pH 7.4. This highlights the scaling of the temperature effect over an extensive range of pCO₂ and the importance of
414 simultaneously studying the impact of these two factors on DMS production. As observed at 10 °C, both the average and the
415 peak DMS concentrations decreased linearly as pCO₂ increased in the warm treatment (Figs. 3d, 4b; Tables 1 and 2).
416 Nevertheless, the pCO₂-induced decrease in DMS concentrations at 15 °C cannot be directly attributed to a decrease in DMSP_t
417 concentrations given that an increase in pCO₂ had no discernable effect on DMSP_t concentrations. In contrast to our
418 observations at the in situ temperature, where DMSP_t continued to increase until day 12, DMSP_t concentrations typically
419 decreased from day 8 and onward (Fig. 3a). This loss in DMSP_t suggests that microbial consumption of DMSP exceeded
420 DMSP algal synthesis. In light of the dominance of *S. costatum*, a phytoplankton taxon not known to exhibit DLA, the bulk of
421 microbial DMSP mediation was likely associated with heterotrophic bacteria. In support of this hypothesis, the bacterial
422 production was ~2 times higher at 15 than at 10 °C between days 8–13 ($19 \pm 1 \mu\text{g C L}^{-1} \text{d}^{-1}$ vs $9.3 \pm 0.9 \mu\text{g C L}^{-1} \text{d}^{-1}$) (Fig. 2),
423 and we observed a significant correlation between the quantity of DMSP_t lost during Phase II (day of the DMSP_t peak
424 concentration to day 13) and the quantity of DMS produced during the same period (coefficient of determination, $r^2 = 0.60$,
425 $p < 0.01$, $n = 11$). Assuming that all the DMSP_t lost was transformed into DMS by bacteria, we calculated that DMS yields
426 could have varied by 0.5 to 32 % across the pCO₂ gradient (mean = 13 ± 11 %). These very rough estimates of DMS yields
427 are likely at the lower end since measured DMS concentrations also reflect losses of DMS through photo-oxidation and
428 bacterial consumption. Nevertheless, we cannot exclude the possibility of some passive uptake of DMSP by the
429 picocyanobacterial population in the mesocosms, although this pathway is not considered to be significant in natural systems
430 (Malmstrom et al., 2005; Vila-Costa et al., 2006a) and does not lead to the production of DMS. Our ‘minimum community’
431 DMS yield estimates agree with an expected range of microbial DMS yields in natural environments, from 2 % to 45 % (see
432 review table in Lizotte et al., 2017). These gross but realistic estimates of heterotrophic bacterial DMSP-to-DMS conversions
433 could explain the bulk of the DMS present in our study, a hypothesis also supported by the strong positive correlation ($r^2 = 0.64$,
434 $p < 0.001$, $n = 70$) between overall DMS concentrations and bacterial production rates. Combined, these findings reinforce the
435 idea that bacterial metabolism, rather than bacterial stocks, may significantly affect the fate of DMSP (Malmstrom et al., 2004a,
436 2004b, 2005; Vila et al., 2004; Vila-Costa et al., 2007; Royer et al., 2010; Lizotte et al., 2017) and that drivers of environmental
437 change, such as temperature and pH, that can alter bacterial activity and strongly impact the gross and net production of DMS.
438 Specific measurements of bacterial DMSP uptake and DMS yields using ³⁵S-DMSP_d should be conducted to assess the impacts
439 of pCO₂ and temperature on the microbial fate of DMSP.

440 4.4 Limitations

441 During our study, the pCO₂ changes were applied abruptly, over a day, from in situ values to pCO₂ levels exceeding the most
442 pessimistic pCO₂ scenarios for the end of the century. Compared to our manipulation, ocean acidification will proceed at a
443 slower temporal scale, potentially allowing species to adapt and evolve to these changing conditions (Stillman and Paganini,
444 2015; Schlüter et al., 2016). However, in the LSLE, the upwelling of low oxygenated waters can rapidly reduce the pH_T to



445 ~7.62, or even lower with contributions of low pH_T (7.12) freshwaters from the Saguenay River during the spring freshet
446 (Mucci et al., 2017). Thus, the swift and extensive pCO_2 range deployed in our experiment may seem improbable for the open
447 ocean on the short term, but may not be inconceivable for this coastal region. However, the warming of 5 °C used in this
448 mesocosm study possibly exceeds the upper limit of temperature increase for the end of the century in this region. In the
449 adjacent Gulf of St. Lawrence (GSL), surface waters temperature (SST) correlates strongly with air temperature, allowing the
450 estimation of past SST. This relationship showed that SST has increased in the GSL by 0.9 °C per century since 1873 (Galbraith
451 et al., 2012), although additional positive anomalies of 0.25–0.75 °C per decade have been shown between 1985 and 2013
452 (Galbraith et al., 2016). In the LSLE, the highest temperatures occur at the end of summer / early fall, and gradually dissipate
453 by heating the subjacent cold intermediate layer through vertical mixing (Cyr et al., 2011). The extent of the projected warming
454 in the LSLE is unknown, but will likely result from the multifaceted interactions between heat transfer from the air and physical
455 factors controlling the water masses.

456 The results from our study could also be influenced by the absence of macrograzers in the mesocosms. An additional grazing
457 pressure could limit the growth of the blooming species, reducing the amount of DMSP produced or could increase the release
458 of DMSP_d through sloppy feeding after the initial bloom (Lee et al., 2003). It is unclear how an increase in grazing pressure
459 would have impacted the concentrations of DMS in our experiment. On the one hand, increased predation could have limited
460 the net accumulation of DMSP_p , with a possible reduction in DMS production. On the other hand, increased grazing could
461 have favoured the release of DMSP_p as DMSP_d , thus increasing the availability of this substrate for microbial uptake,
462 mediation and possible conversion into DMS. Despite the absence of reported changes in community composition in our study,
463 many OA mesocosm experiments have described changes in DMS concentrations associated with shifts in community
464 structure in the past (Vogt et al., Hopkins et al., 2010; Kim et al., 2010, Park et al., 2014, Webb et al., 2015). Nonetheless, our
465 results align with those of other OA studies (Archer et al., 2013; Hussherr et al., 2017), suggesting that the mediation of
466 heterotrophic bacteria plays a major role in DMS cycling in the absence of reported phytoplanktonic DLA, such as in a diatom
467 dominated bloom in the LSLE.

468 5. Conclusions

469 The objective of this study was to quantify the combined impact of increases in pCO_2 and temperature on the dynamics of
470 DMS during a fall diatom bloom in the St. Lawrence Estuary. Our mesocosm experiment allowed us to capture the
471 development and declining phases of a bloom strongly dominated by the diatom *Skeletonema costatum* and the related changes
472 in bacterial abundance and production. As expected, warming accelerated the development of the bloom, but also its decline.
473 Both DMSP_i and DMS concentrations increased during the development phase of the bloom, but peak concentrations were
474 reached as the bloom was declining. Increasing pCO_2 had no discernable effect on the total amount of DMSP_i produced at both
475 temperatures tested. In contrast, increasing the pCO_2 to the value forecasted for the end of this century resulted in a linear
476 decrease in DMS concentrations by 33 % and by as much as 69 % over the full pCO_2 gradient tested. These results are



477 consistent with previous reports that acidification has a greater impact on the processes that control the conversion of DMSP
478 to DMS than on the production of DMSP itself. The pCO₂-induced decrease in DMS concentrations observed in this study
479 adds to the bulk of previous studies reporting a similar trend. In diatom dominated systems, such as the one under study in this
480 experiment, heterotrophic processes underlying DMS production seem to be most sensitive to modifications in pCO₂. Whereas
481 predatory grazing and its associated impacts on DMS production cannot be ruled out entirely, the decreases in DMS
482 concentrations in response to heightened pCO₂ are likely related to reductions in bacterial-mediated DMS production, a
483 hypothesis partly supported by the significant positive correlations found between bacterial production rates and DMS
484 concentrations. Whereas the DMS concentrations decreased significantly with increasing pCO₂ at both 10 °C and 15 °C,
485 warming the mesocosms by 5 °C translated into a positive offset in concentrations of DMS over the whole range of pCO₂
486 tested. Higher DMSP release and increased bacterial productivity in the warm treatment partially explain the stimulating effect
487 of temperature on DMS net production. Overall, results from this full factorial mesocosm experiment suggest that warming
488 could mitigate the expected reduction in DMS production due to ocean acidification, even increasing the net DMS production
489 with the potential to curtail radiative forcing.

490

491 *Data availability.* The data have been submitted to be freely accessible via Pangaea or can be obtained by contacting the author
492 (robin.benard.1@ulaval.ca).

493 *Author contributions.* R. Bénard was responsible for the experimental design elaboration, data sampling and processing, and
494 the writing of this article. Several co-authors supplied specific data included in this article, and all co-authors contributed to
495 this final version of the article.

496 *Competing interests.* The authors declare that they have no conflict of interest.

497 **Acknowledgements**

498 The authors wish to thank the Station Aquicole-ISMER, particularly Nathalie Morin and her staff, for their support during the
499 mesocosm experiment. We also wish to acknowledge Gilles Desmeules, Bruno Cayouette, Sylvain Blondeau, Claire Lix,
500 Rachel Husserr, Liliane St-Amand, Marjolaine Blais, Armelle Galine Simo Matchim and Marie-Amélie Blais for their
501 precious help over the duration of the experiment. This study was funded by a Team grant from the Fonds de recherche du
502 Québec – Nature et technologies (FRQNT-Équipe-165335), the Canada Foundation for Innovation, the Canada Research Chair
503 on Ocean Biogeochemistry and Climate, and by Fisheries and Oceans Canada. This is a contribution to the research program
504 of Québec-Océan.

505 **References**

506 Andreae, M. O.: Ocean-atmosphere interactions in the global biogeochemical sulfur cycle, *Mar. Chem.*, 30, 1–3, 1990.



- 507 Andreae, M.O. and Crutzen, P. J.: Atmospheric aerosols: biogeochemical sources and role in atmospheric chemistry, *Science*,
508 276(5315), 1052–1058, doi:10.1126/science.276.5315.1052, 1997.
- 509 Annane, S., St-Amand, L., Starr, M., Pelletier, E., and Ferreyra, G. A.: Contribution of transparent exopolymeric particles
510 (TEP) to estuarine particulate organic carbon pool, *Mar. Ecol. Prog. Ser.*, 529, 17–34, doi:10.3354/meps11294, 2015.
- 511 Avgoustidi, V., Nightingale, P. D., Joint, I., Steinke, M., Turner, S. M., Hopkins, F. E., and Liss, P. S.: Decreased marine
512 dimethyl sulfide production under elevated CO₂ levels in mesocosm and in vitro studies, *Environ. Chem.*, 9(4), 399,
513 doi:10.1071/EN1125, 2012.
- 514 Barnard, W.R., Andreae, M.O., Watkins, W.E., Bingemer, H., and Georgii, H.W.: The flux of dimethylsulfide from the oceans
515 to the atmosphere. *J. Geophys. Res.*, 87(C11), 8787–8793, 1982.
- 516 Bates, T. S., Lamb, B. K., Guenther, A., Dignon, J., and Stoiber, R. E.: Sulfur emissions to the atmosphere from natural sources,
517 *J. Atmos. Chem.*, 14(1–4), 315–337, doi:10.1007/BF00115242, 1992.
- 518 Bell, R. T.: Estimating production of heterotrophic bacterioplankton via incorporation of tritiated thymidine, in: *Handbook of*
519 *methods in aquatic microbial ecology*, Eds: Kemp, P. F., Sherr, B. F., Sherr, E. B., and Cole, J., Lewis Publisher, Boca Raton,
520 495–503, 1993.
- 521 Belzile, C., Brugel, S., Nozais, C., Gratton, Y. and Demers, S.: Variations of the abundance and nucleic acid content of
522 heterotrophic bacteria in Beaufort Shelf waters during winter and spring, *J. Mar. Syst.*, 74(3–4), 946–956,
523 doi:10.1016/j.jmarsys.2007.12.010, 2008.
- 524 B nard, R., L vasseur, M., Scarratt, M. G., Blais, M.-A., Mucci, A., Ferreyra, G., Starr, M., Gosselin, M., Tremblay, J.- ., and
525 Lizotte, M.: Experimental assessment of the sensitivity of an estuarine phytoplankton fall bloom to acidification and warming,
526 *Biogeosciences Discuss.*, <https://doi.org/10.5194/bg-2018-31>, accepted, 2018.
- 527 Boyd, P. W., Lennartz, S. T., Glover, D. M. and Doney, S. C.: Biological ramifications of climate-change-mediated oceanic
528 multi-stressors, *Nat. Clim. Chang.*, 5(1), 71–79, doi:10.1038/nclimate2441, 2015.
- 529 Boyd, P. W., Collins, S., Dupont, S., Fabricius, K., Gattuso, J.-P., Havenhand, J., Hutchins, D. A., Riebesell, U., Rintoul, M.
530 S., Vichi, M., Biswas, H., Ciotti, A., Gao, K., Gehlen, M., Hurd, C. L., Kurihara, H., McGraw, C. M., Navarro, J. M., Nilsson,
531 G. E., Passow, U. and P rtner, H.-O.: Experimental strategies to assess the biological ramifications of multiple drivers of
532 global ocean change-A review, *Glob. Chang. Biol.*, 24(6), 2239–2261, doi:10.1111/gcb.14102, 2018.
- 533 Brimblecombe, P., and Shooter, D.: Photo-oxidation of dimethylsulphide in aqueous solution, *Mar. Chem.*, 19, 343–353, 1986.
- 534 Byrne, R. H.: Standardization of Standard Buffers by Visible Spectrometry, *Anal. Chem.*, 59, 1479–1481,
535 doi:10.1021/ac00137a025, 1987.
- 536 Caldeira, K., and Wickett, M. E.: Ocean model predictions of chemistry changes from carbon dioxide emissions to the
537 atmosphere and ocean, *J. Geophys. Res.*, 110(C9), 1–12, doi:10.1029/2004JC002671, 2005.
- 538 Cai, W. J., and Wang, Y.: The chemistry, fluxes, and sources of carbon dioxide in the estuarine waters of the Satilla and
539 Altamaha Rivers, Georgia, *Limnol. Oceanogr.*, 43(4), 657–668, doi:10.4319/lo.1998.43.4.0657, 1998.



- 540 Cantin, G., Levasseur, M., Gosselin, M., Michaud, S.: Role of zooplankton in the mesoscale distribution of surface
541 dimethylsulfide concentrations in the Gulf of St. Lawrence, Canada, *Mar. Ecol. Prog. Ser.*, 141, 103-117, 1996.
- 542 Cantoni, G. L. and Anderson, D. Enzymatic cleavage of dimethylpropiothetin by *Polysiphonia Lanosa*, *J. Bio. Chem.*, 222,
543 171-177, 1956.
- 544 Carslaw, K. S., Boucher, O., Spracklen, D. V., Mann, G. W., Rae, J. G. L., Woodward, S., and Kulmala, M.: A review of
545 natural aerosol interactions and feedbacks within the Earth system, *Atmos. Chem. Phys.*, 10, 1701–1737, doi:10.5194/acp-10-
546 1701-2010, 2010.
- 547 Charlson, R., Lovelock, J., Andreae, M., and Warren, S.: Oceanic phytoplankton, atmospheric sulphur, cloud albedo and
548 climate, *Nature*, 326, 656–661, 1987.
- 549 Clayton, T. D., and Byrne, R. H.: Spectrophotometric seawater pH measurements: total hydrogen ion concentration scale
550 calibration of m-cresol purple and at-sea results, *Deep. Res. Part I*, 40(10), 2115–2129, doi:10.1016/0967-0637(93)90048-8,
551 1993.
- 552 Cyr, F., Bourgault, D., and Galbraith, P. S.: Interior versus boundary mixing of a cold intermediate layer, *J. Geophys. Res.*
553 *Ocean.*, 116(12), 1–12, doi:10.1029/2011JC007359, 2011.
- 554 Dacey, J. W. H., and Wakeham, S. G.: Oceanic dimethylsulfide: production during zooplankton grazing, *Science*, 233, 1314–
555 1316, 1986.
- 556 Dickson, A. G.: Standard potential of the reaction: $\text{AgCl(s)} + 1/2\text{H}_2(\text{g}) = \text{Ag(s)} + \text{HCl(aq)}$ and the standard acidity constant of
557 the ion HSO_4^- in synthetic sea water from 273.15 to 318.15 K, *J. Chem. Thermodyn.*, 22(2), 113–127, doi:10.1016/0021-
558 9614(90)90074-Z, 1990.
- 559 Doney, S. C., Fabry, V. J., Feely, R. A., and Kleypas, J. A.: Ocean acidification: The other CO₂ problem, *Ann. Rev. Mar. Sci.*,
560 1(1), 169–192, doi:10.1146/annurev.marine.010908.163834, 2009.
- 561 Engel, A., Delille, B., Jacquet, S., Riebesell, U., Rochelle-Newall, E., Terbrüggen, A., and Zondervan, I.: Transparent
562 exopolymer particles and dissolved organic carbon production by *Emiliania huxleyi* exposed to different CO₂ concentrations:
563 A mesocosm experiment, *Aquat. Microb. Ecol.*, 34(1), 93–104, doi:10.3354/ame034093, 2004a.
- 564 Engel, A., Thoms, S., Riebesell, U., Rochelle-Newall, E., and Zondervan, I.: Polysaccharide aggregation as a potential sink of
565 marine dissolved organic carbon, *Nature*, 428(6986), 929–932, doi:10.1038/nature02453, 2004b.
- 566 Engel, A., Piontek, J., Grossart, H.-P., Riebesell, U., Schulz, K. G., and Sperling, M.: Impact of CO₂ enrichment on organic
567 matter dynamics during nutrient induced coastal phytoplankton blooms, *J. Plankton Res.*, 36(3), 641–657,
568 doi:10.1093/plankt/fbt125, 2014.
- 569 Feely, R. A., Doney, S. C., and Cooley, S. R.: Ocean Acidification: Present Conditions and Future Changes in a High-CO₂
570 World, *Oceanography*, 22(4), 36–47, doi:DOI 10.5670/oceanog.2009.95, 2009.
- 571 Fuhrman, J. A., and Azam, F.: Bacterioplankton secondary production estimates for coastal waters of British Columbia,
572 Antarctica, and California, *Appl. Environ. Microbiol.*, 39(6), 1085–1095, 1980.



- 573 Fuhrman, J. A., and Azam, F.: Thymidine incorporation as a measure of heterotrophic bacterioplankton production in marine
574 surface waters: Evaluation and field results, *Mar. Biol.*, 66(2), 109–120, doi:10.1007/BF00397184, 1982.
- 575 Gaaloul, H.: Effets du changement global sur les particules exopolymériques transparentes au sein de l'estuaire maritime du
576 Saint-Laurent, M.Sc. thesis, Université du Québec à Rimouski, Canada, 133 pp., 2017.
- 577 Galbraith, P. S., Chassé, J., Gilbert, D., Larouche, P., Brickman, D., Pettigrew, B., Devine, L., Gosselin, A., Pettipas, R. G.,
578 and Lafleur, C.: Physical Oceanographic Conditions in the Gulf of St. Lawrence in 2011, *DFO Can. Sci. Advis. Sec. Res.*
579 *Doc.*, 2012/023, iii + 85 pp, 2012.
- 580 Galbraith, P. S., Chassé, J., Caverhill, C., Nicot, P., Gilbert, D., Pettigrew, B., Lefavre, D., Brickman, D., Devine, L., and
581 Lafleur, C.: Physical Oceanographic Conditions in the Gulf of St. Lawrence in 2015, *DFO Can. Sci. Advis. Sec. Res. Doc.*,
582 2016/056, v + 90 pp, 2016.
- 583 Gattuso, J.-P., Magnan, A., Bille, R., Cheung, W. W. L., Howes, E. L., Joos, F., Allemand, D., Bopp, L., Cooley, S. R., Eakin,
584 C. M., Hoegh-Guldberg, O., Kelly, R. P., Portner, H.-O., Rogers, a. D., Baxter, J. M., Laffoley, D., Osborn, D., Rankovic, A.,
585 Rochette, J., Sumaila, U. R., Treyer, S., and Turley, C.: Contrasting futures for ocean and society from different anthropogenic
586 CO₂ emissions scenarios, *Science*, 349(6243), doi:10.1126/science.aac4722, 2015.
- 587 Green, D.H., Shenoy, D. M., Hart, M. C., and Hatton, A. D.: Coupling of dimethylsulfide oxidation to biomass production by
588 a marine Flavobacterium, *Appl. Environ. Microbiol.*, 77(9), 3137–3140, doi:10.1128/AEM.02675-10, 2011.
- 589 Grossart, H.-P., Allgaier, M., Passow, U., and Riebesell, U.: Testing the effect of CO₂ concentration on the dynamics of marine
590 heterotrophic bacterioplankton, *Limnol. Oceanogr.*, 51(1), 1–11, doi:10.4319/lo.2006.51.1.0001, 2006.
- 591 Gunderson, A. R., Armstrong, E. J., and Stillman, J. H.: Multiple Stressors in a Changing World: The Need for an Improved
592 Perspective on Physiological Responses to the Dynamic Marine Environment, *Ann. Rev. Mar. Sci.*, 8(1), 357–378,
593 doi:10.1146/annurev-marine-122414-033953, 2016.
- 594 Hansen, H. P., and Koroleff, F.: Determination of nutrients, in: *Methods of Seawater Analysis*, 3, Eds: Grasshoff K., Kremling,
595 K., and Ehrhardt, M., Wiley-VCH Verlag GmbH, Weinheim, Germany, 159–228, doi:10.1002/9783527613984.ch10, 2007.
- 596 Hatton, A. D., Darroch, L., and Malin, G.: The role of dimethylsulphoxide in the marine biogeochemical cycle of
597 dimethylsulphide, *Oceanogr. Mar. Biol. An Annu. Rev.*, 42, 29–56, 2004.
- 598 Hopkins, F. E., and Archer, S. D.: Consistent increase in dimethyl sulfide (DMS) in response to high CO₂ in five shipboard
599 bioassays from contrasting NW European waters, *Biogeosciences*, 11(18), 4925–4940, doi:10.5194/bg-11-4925-2014, 2014.
- 600 Hopkins, F. E., Turner, S. M., Nightingale, P. D., Steinke, M., Bakker, D., and Liss, P. S.: Ocean acidification and marine
601 trace gas emissions, *Proc. Natl. Acad. Sci.*, 107(2), 760–765, doi:10.1073/pnas.0907163107, 2010.
- 602 Hussherr, R., Levasseur, M., Lizotte, M., Tremblay, J. É., Mol, J., Thomas, H., Gosselin, M., Starr, M., Miller, L. A., Jarniková,
603 T., Schuback, N., and Mucci, A.: Impact of ocean acidification on Arctic phytoplankton blooms and dimethyl sulfide
604 concentration under simulated ice-free and under-ice conditions, *Biogeosciences*, 14(9), 2407–2427, doi:10.5194/bg-14-2407-
605 2017, 2017.



- 606 IPCC: Working Group I Contribution to the Fifth Assessment Report Climate Change 2013: The Physical Science Basis,
607 Intergov. Panel Clim. Chang., 1535, doi:10.1017/CBO9781107415324., 2013.
- 608 Iverson, R. L., Nearhoof, F. L. and Andreae, M. O.: Production of dimethylsulfonium propionate and dimethylsulfide by
609 phytoplankton in estuarine and coastal waters, *Limnol. Oceanogr.*, 34(1), 53–67, doi:10.4319/lo.1989.34.1.0053, 1989.
- 610 Karsten, U., Kück, K., Vogt, C., and Kirst, G. O.: Dimethylsulfoniopropionate production in phototrophic organisms and its
611 physiological functions as a cryoprotectant, in: *Biological and environmental chemistry of DMSP and related sulfonium*
612 *compounds*, Eds: Kiene, R. P., Visscher, P. T., Keller, M. D., and Kirst, G. O., Springer US, Boston, MA, 143–153,
613 doi:10.1007/978-1-4613-0377-0, 1996.
- 614 Keller, M. D.: Dimethyl sulfide production and marine phytoplankton: the importance of species composition and cell size,
615 *Biol. Oceanogr.*, 6(5–6), 375–382, doi:10.1080/01965581.1988.10749540, 1989.
- 616 Kettle, A. J., Andreae, M. O., Amouroux, D., Andreae, T. W., Bates, T. S., Berresheim, H., Bingemer, H., Boniforti, R., Curran,
617 M. A. J., diTullio, G. R., Helas, G., Jones, G. B., Keller, I. M. D., Kiene, R. P., Leck, C., Levasseur, M., Maspero, M., Matrai,
618 P., McTaggart, A. R., Mihalopoulos, N., Nguyen, B. C., Novo, A., Putaud, J. P., Rapsomanikis, S., Roberts, G., Schebeske,
619 G.; Sharma, S., Simó, R., Staubes, R., Turner, S., and Uher, G.: A global database of sea surface dimethylsulfide (DMS)
620 measurements and a procedure to predict sea surface DMS as a function of latitude, longitude, and month, *Global Biogeochem.*
621 *Cycles*, 13, 399–444, 1999.
- 622 Kettles, N. L., Kopriva, S., and Malin, G.: Insights into the regulation of DMSP synthesis in the diatom *Thalassiosira*
623 *pseudonana* through APR activity, proteomics and gene expression analyses on cells acclimating to changes in salinity, light
624 and nitrogen, *PLoS One*, 9(4), doi:10.1371/journal.pone.0094795, 2014.
- 625 Kiene, R. P., Linn, L. J.: Distribution and turnover of dissolved DMSP and its relationship with bacterial production and
626 dimethylsulfide in the Gulf of Mexico, *Limnol. Oceanogr.*, 45, 849–861, 2000.
- 627 Kiene, R. P., and Service, S. K.: Decomposition of dissolved DMSP and DMS in estuarine waters: dependence on temperature
628 and substrate concentration, *Mar. Ecol. Prog. Ser.*, 76, 1–11, 1991.
- 629 Kiene, R. P., Linn, L. J., Gonzalez, J., Moran, M. A., and Bruton, J. A.: Dimethylsulfoniopropionate and methanethiol are
630 important precursors of methionine and protein-sulfur in marine bacterioplankton, *Appl Environ. Microbiol.*, 65, 4549–4558,
631 1999.
- 632 Kiene, R. P., Linn, L. J., and Bruton, J. A. New and important roles for DMSP in marine microbial communities, *J. Sea. Res.*,
633 43, 209–224, 2000.
- 634 Kim, K. Y., Garbary, D. J., and McLachlan, J. L.: Phytoplankton dynamics in Pomquet Harbour, Nova Scotia: a lagoon in the
635 southern Gulf of St Lawrence, *Phycologica*, 43(3), 311–328, 2004.
- 636 Kim, J. M., Lee, K., Yang, E. J., Shin, K., Noh, J. H., Park, K. T., Hyun, B., Jeong, H. J., Kim, J. H., Kim, K. Y., Kim, M.,
637 Kim, H. C., Jang, P. G. and Jang, M. C.: Enhanced production of oceanic dimethylsulfide resulting from CO₂-induced grazing
638 activity in a high CO₂ world, *Environ. Sci. Technol.*, 44(21), 8140–8143, doi:10.1021/es102028k, 2010.



- 639 Kirst, G. O., Thiel, C., Wolff, H., Nothnagel, J., Wanzek M., and Ulmke, R.: Dimethylsulfoniopropionate (DMSP) in ice-algae
640 and its possible biological role, *Mar. Chem.*, 35, 381–388, 1991.
- 641 Kwint, R. L., and Kramer, K. J.: Dimethylsulphide production by plankton communities, *Mar. Ecol. Prog. Ser.*, 121(1–3),
642 227–238, doi:10.3354/meps121227, 1995.
- 643 Hill, R. W., White, B. A., Cottrell, M. T., Dacey, J. W. H.: Virus-mediated total release of dimethylsulfoniopropionate from
644 marine phytoplankton: a potential climate process, *Aquat. Microb. Ecol.*, 14, 1–6, 1998.
- 645 Lana, A., Bell, T. G., Simó, R., Vallina, S. M., Ballabrera-Poy, J., Kettle, a. J., Dachs, J., Bopp, L., Saltzman, E. S., Stefels, J.,
646 Johnson, J. E., and Liss, P. S.: An updated climatology of surface dimethylsulfide concentrations and emission fluxes in the
647 global ocean, *Global Biogeochem. Cycles*, 25(1), 1–17, doi:10.1029/2010GB003850, 2011.
- 648 Laroche, D., Vézina, A. F., Levasseur, M., Gosselin, M., Stefels, J., Keller, M. D., Matrai, P. A., and Kwint, R. L. J.: DMSP
649 synthesis and exudation in phytoplankton: A modeling approach, *Mar. Ecol. Prog. Ser.*, 180(May), 37–49,
650 doi:10.3354/meps180037, 1999.
- 651 Lee, P. A., Saunders, P. A., De Mora, S. J., Deibel, D. and Levasseur, M.: Influence of copepod grazing on concentrations of
652 dissolved dimethylsulfoxide and related sulfur compounds in the North Water, Northern Baffin Bay, *Mar. Ecol. Prog. Ser.*,
653 255, 235–248, doi:10.3354/meps255235, 2003.
- 654 Lee, P. A., Rudisill, J. R., Neeley, A. R., Maucher, J. M., Hutchins, D. A., Feng, Y., Hare, C. E., Leblanc, K., Rose, J. M.,
655 Wilhelm, S. W., Rowe, J. M., and Giacomo, R.: Effects of increased pCO₂ and temperature on the North Atlantic spring bloom.
656 III. Dimethylsulfoniopropionate, *Mar. Ecol. Prog. Ser.*, 388, 41–49, doi:10.3354/meps08135, 2009.
- 657 Le Quéré, C., Andres, R. J., Boden, T., Conway, T., Houghton, R. A., House, J. I., Marland, G., Peters, G. P., Van Der Werf,
658 G. R., Ahlström, A., Andrew, R. M., Bopp, L., Canadell, J. G., Ciais, P., Doney, S. C., Enright, C., Friedlingstein, P.,
659 Huntingford, C., Jain, A. K., Jourdain, C., Kato, E., Keeling, R. F., Klein Goldewijk, K., Levis, S., Levy, P., Lomas, M.,
660 Poulter, B., Raupach, M. R., Schwinger, J., Sitch, S., Stocker, B. D., Viovy, N., Zaehle, S., and Zeng, N.: The global carbon
661 budget 1959–2011, *Earth Syst. Sci. Data*, 5(1), 165–185, doi:10.5194/essd-5-165-2013, 2013.
- 662 Le Quéré, C., Moriarty, R., andrew, R. M., Canadell, J. G., Sitch, S., Korsbakken, J. I., Friedlingstein, P., Peters, G. P., andres,
663 R. J., Boden, T. A., Houghton, R. A., House, J. I., Keeling, R. F., Tans, P., Arneeth, A., Bakker, D. C. E., Barbero, L., Bopp,
664 L., Chang, J., Chevallier, F., Chini, L. P., Ciais, P., Fader, M., Feely, R. A., Gkritzalis, T., Harris, I., Hauck, J., Ilyina, T., Jain,
665 A. K., Kato, E., Kitidis, V., Klein Goldewijk, K., Koven, C., Landschützer, P., Lauvset, S. K., Lefèvre, N., Lenton, A., Lima,
666 I. D., Metzl, N., Millero, F., Munro, D. R., Murata, A., S. Nabel, J. E. M., Nakaoka, S., Nojiri, Y., O’Brien, K., Olsen, A.,
667 Ono, T., Pérez, F. F., Pfeil, B., Pierrot, D., Poulter, B., Rehder, G., Rödenbeck, C., Saito, S., Schuster, U., Schwinger, J.,
668 Séférian, R., Steinhoff, T., Stocker, B. D., Sutton, A. J., Takahashi, T., Tilbrook, B., Van Der Laan-Luijkx, I. T., Van Der
669 Werf, G. R., Van Heuven, S., Vandemark, D., Viovy, N., Wiltshire, A., Zaehle, S., and Zeng, N.: Global Carbon Budget 2015,
670 *Earth Syst. Sci. Data*, 7(2), 349–396, doi:10.5194/essd-7-349-2015, 2015.



- 671 Levasseur, M., Michaud, S., Egge, J., Cantin, G., Nejstgaard, J. C., Sanders, R., Fernandez, E., Solberg, P. T., Heimdal, B.,
672 and Gosselin, M.: Production of DMSP and DMS during a mesocosm study of an *Emiliania huxleyi* bloom: Influence of
673 bacteria and *Calanus finmarchicus* grazing, *Mar. Biol.*, 126(4), 609–618, doi:10.1007/BF00351328, 1996.
- 674 Liss, P. S. and Lovelock, J. E.: Climate change: The effect of DMS emissions, *Environ. Chem.*, 4(6), 377–378,
675 doi:10.1071/EN07072, 2007.
- 676 Lizotte, M., Levasseur, M., Michaud, S., Scarratt, M. G., Merzouk, A., Gosselin, M., Pommier, J., Rivkin, R. B., and Kiene,
677 R. P.: Macroscale patterns of the biological cycling of dimethylsulfoniopropionate (DMSP) and dimethylsulfide (DMS) in the
678 Northwest Atlantic, *Biogeochemistry*, 110(1–3), 183–200, doi:10.1007/s10533-011-9698-4, 2012.
- 679 Lizotte, M., Levasseur, M., Law, C. S., Walker, C. F., Safi, K. A., Marriner, A. and Kiene, R. P.: Dimethylsulfoniopropionate
680 (DMSP) and dimethyl sulfide (DMS) cycling across contrasting biological hotspots of the New Zealand subtropical front,
681 *Ocean Sci.*, 13(6), 961–982, doi:10.5194/os-13-961-2017, 2017.
- 682 Lovelock, J. E., Maggs, R. J., and Rasmussen R. A.: Atmospheric dimethyl sulfide and natural sulfur cycle, *Nature*, 237(5356),
683 452–453, 1972.
- 684 Malin, G., and Kirst, G. O.: Algal production of dimethyl sulfide and its atmospheric role, *J. Phycol.*, 33, 889–896, 1997.
- 685 Malin, G., Wilson, W. H., Bratbak, G., Liss, P. S., and Mann, N. H.: Elevated production of dimethylsulfide resulting from
686 viral infection of cultures of *Phaeocystis pouchetii*, *Limnol. Oceanogr.*, 43(6), 1389–1393, doi:10.4319/lo.1998.43.6.1389,
687 1998.
- 688 Malmstrom, R. R., Kiene, R. P., Cottrell, M. T., and Kirchman, D. L.: Contribution of SAR11 bacteria to dissolved
689 dimethylsulfoniopropionate and amino acid uptake in the north Atlantic Ocean, *Appl. Environ. Microbiol.*, 70(7), 4129–4135,
690 doi:10.1128/AEM.70.7.4129, 2004a.
- 691 Malmstrom, R. R., Kiene, R. P., and Kirchman, D. L.: Identification and enumeration of bacteria assimilating
692 dimethylsulfoniopropionate (DMSP) in the North Atlantic and Gulf of Mexico, *Limnol. Oceanogr.*, 49, 597–606, doi:
693 10.4319/lo.2004.49.2.0597, 2004b.
- 694 Malmstrom, R. R., Kiene, R. P., Vila, M., and Kirchman, D. L.: Dimethylsulfoniopropionate (DMSP) assimilation by
695 *Synechococcus* in the Gulf of Mexico and northwest Atlantic Ocean, *Limnol. Oceanogr.*, 50(6), 1924–1931,
696 doi:10.4319/lo.2005.50.6.1924, 2005.
- 697 Marie, D., Simon, N., and Vaulot, D.: Phytoplankton cell counting by flow cytometry, *Algal Cult. Tech.*, 253–267,
698 doi:10.1016/B978-012088426-1/50018-4, 2005.
- 699 Mucci, A., Levasseur, M., Gratton, Y., Martias, C., Scarratt, M., Gilbert, D., Tremblay, J.-É., Ferreyra, G., and Lansard, B.:
700 Tidally-induced variations of pH at the head of the Laurentian Channel, *Can. J. Fish. Aquat. Sci.*, doi:10.1139/cjfas-2017-
701 0007, 2017.
- 702 Nguyen, B. C., Belviso, S., Mihalopoulos, N., Gostan, J., Nival, P.: Dimethyl sulfide production during natural phytoplankton
703 blooms, *Mar. Chem.*, 24, 133–141, 1988



- 704 Nightingale, P.D., Malin, G., Law, C.S., Watson, A.J., Liss, P.S., Liddicoat, M.I., Boutin, J., Upstill-Goddard, R.C.: In situ
705 evaluation of air–sea gas exchange parameterizations using novel conservative and volatile tracers, *Global Biogeochem.*
706 *Cycles*, 14 (1), 373–387, 2000.
- 707 Niki, T., Kunugi, M., and Otsuki, A.: DMSP-lyase activity in five marine phytoplankton species: Its potential importance in
708 DMS production, *Mar. Biol.*, 136(5), 759–764, doi:10.1007/s002279900235, 2000.
- 709 Park, K. T., Lee, K., Shin, K., Yang, E. J., Hyun, B., Kim, J. M., Noh, J. H., Kim, M., Kong, B., Choi, D. H., Choi, S. J., Jang,
710 P. G., and Jeong, H. J.: Direct linkage between dimethyl sulfide production and microzooplankton grazing, resulting from prey
711 composition change under high partial pressure of carbon dioxide conditions, *Environ. Sci. Technol.*, 48(9), 4750–4756,
712 doi:10.1021/es403351h, 2014.
- 713 Parsons, T. R., Maita, Y., and Lalli, C. M.: A manual of chemical and biological methods for seawater analysis, Permagon
714 Press, New York, 1984.
- 715 Paul, C., Sommer, U., Garzke, J., Moustaka-Gouni, M., Paul, A., and Matthiessen, B.: Effects of increased CO₂ concentration
716 on nutrient limited coastal summer plankton depend on temperature, *Limnol. Oceanogr.*, 61(3), 853–868,
717 doi:10.1002/lno.10256, 2016.
- 718 Pierrot, D. E., Lewis, E., and Wallace, D. W. R.: MS Excel program developed for CO₂ system calculations, Carbon Dioxide
719 Information Analysis Center, ONRL/CDIAC-105a, Oak Ridge National Laboratory, US Department of Energy, Oak Ridge,
720 Tennessee, USA, 2006.
- 721 Pinhassi, J., Simó, R., González, J. M., Vila, M., Alonso-Sáez, L., Kiene, R. P., Moran, M. A., and Pedrós-Alió, C.:
722 Dimethylsulfoniopropionate turnover is linked to the composition and dynamics of the bacterioplankton assemblage during a
723 microcosm phytoplankton bloom, *Appl. Environ. Microbiol.*, 71(12), 7650–7660, doi:10.1128/AEM.71.12.7650-7660.2005,
724 2005.
- 725 Quinn, P. K., and Bates, T. S.: The case against climate regulation via oceanic phytoplankton sulphur emissions., *Nature*,
726 480(7375), 51–6, doi:10.1038/nature10580, 2011.
- 727 Quinn, P. K., Coffman, D. J., Johnson, J. E., Upchurch, L. M., and Bates, T. S.: Small fraction of marine cloud condensation
728 nuclei made up of sea spray aerosol, *Nat. Geosci.*, 10(9), 674–679, doi:10.1038/ngeo3003, 2017.
- 729 R Core Team: R: A language and environment for statistical computing. R Foundation for Statistical Computing, Vienna,
730 Austria. URL <https://www.R-project.org/>, 2016.
- 731 Riebesell, U. and Gattuso, J. P.: Lessons learned from ocean acidification research, *Nat. Clim. Chang.*, 5(1), 12–14,
732 doi:10.1038/nclimate2456, 2015.
- 733 Robert-Baldo, G., Morris, M., and Byrne, R.: Spectrophotometric determination of seawater pH using phenol red, *Anal. Chem.*,
734 3(57), 2564–2567, doi:10.1021/ac00290a030, 1985.
- 735 Roemmich, D., Church, J., Gilson, J., Monselesan, D., Sutton, P. and Wijffels, S.: Unabated planetary warming and its ocean
736 structure since 2006, *Nat. Clim. Chang.*, 5(3), 240–245, doi:10.1038/nclimate2513, 2015.



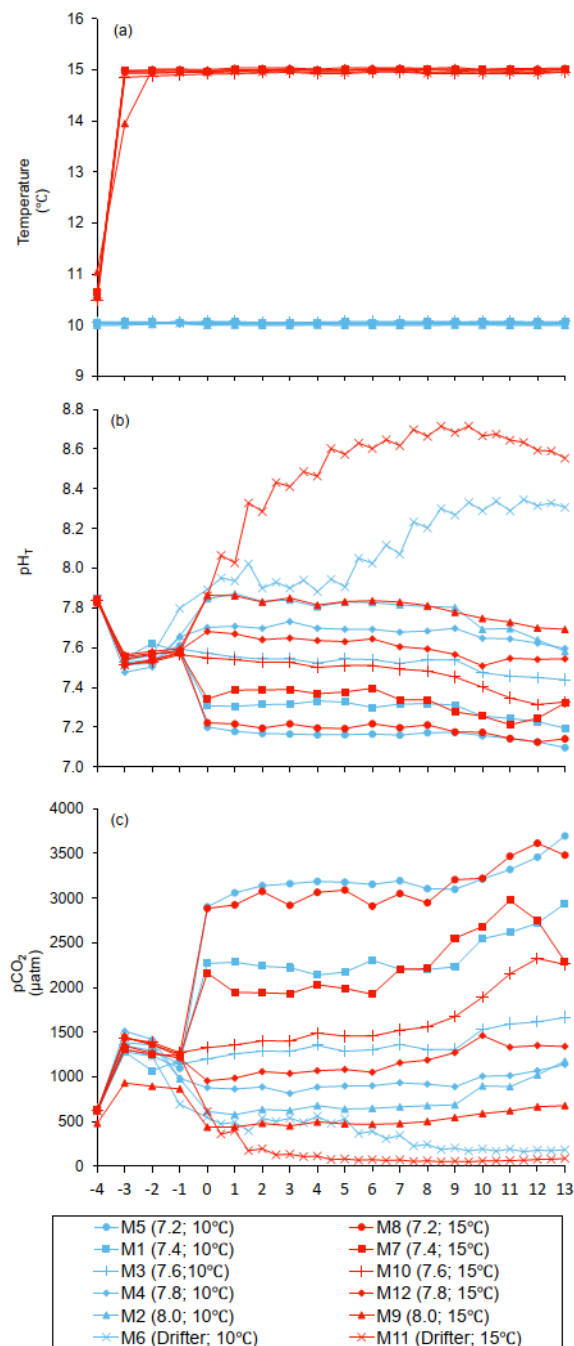
- 737 Ruiz-González, C., Galí, M., Gasol, J. M. and Simó, R.: Sunlight effects on the DMSP-sulfur and leucine assimilation activities
738 of polar heterotrophic bacterioplankton, *Biogeochemistry*, 110(1–3), 57–74, doi:10.1007/s10533-012-9699-y, 2012.
- 739 Scarratt, M. G., Levasseur, M., Schultes, S., Michaud, S., Cantin, G., Vézina, A., Gosselin, M. and De Mora, S. J.: Production
740 and consumption of dimethylsulfide (DMS) in North Atlantic waters, *Mar. Ecol. Prog. Ser.*, 204, 13–26,
741 doi:10.3354/meps204013, 2000.
- 742 Schlüter, L., Lohbeck, K. T., Gröger, J. P., Riebesell, U. and Reusch, T. B. H.: Long-term dynamics of adaptive evolution in
743 a globally important phytoplankton species to ocean acidification, *Sci. Adv.*, 2(7), e1501660–e1501660,
744 doi:10.1126/sciadv.1501660, 2016.
- 745 Schwinger, J., Tjiputra, J., Goris, N., Six, K. D., Kirkevåg, A., Seland, Ø., Heinze, C. and Ilyina, T.: Amplification of global
746 warming through pH dependence of DMS production simulated with a fully coupled Earth system model, *Biogeosciences*,
747 14(15), 3633–3648, doi:10.5194/bg-14-3633-2017, 2017.
- 748 Simó, R.: Production of atmospheric sulfur by oceanic plankton: Biogeochemical, ecological and evolutionary links, *Trends*
749 *Ecol. Evol.*, 16(6), 287–294, doi:10.1016/S0169-5347(01)02152-8, 2001.
- 750 Simó, R.: From cells to globe: approaching the dynamics of DMS(P) in the ocean at multiple scales, *Can. J. Fish. Aquat. Sci.*,
751 61(5), 673–684, doi:10.1139/f04-030, 2004.
- 752 Simó, R., and Pedrós-Alió, C.: Role of vertical mixing in controlling the oceanic production of dimethyl sulphide, *Nature*, 402,
753 396–399, doi:10.1038/46516, 1999.
- 754 Six, K. D., Kloster, S., Ilyina, T., Archer, S. D., Zhang, K., and Maier-Reimer, E.: Global warming amplified by reduced
755 sulphur fluxes as a result of ocean acidification, *Nat. Clim. Chang.*, 3(11), 975–978, doi:10.1038/nclimate1981, 2013.
- 756 Starr, M., St-Amand, L., Devine, L., Bérard-Therriault, L. and Galbraith, P. S.: State of phytoplankton in the Estuary and Gulf
757 of St. Lawrence during 2003, *CSAS Res. Doc.*, 2004/123, 35, 2004.
- 758 Stefels, J.: Physiological aspects of the production and conversion of DMSP in marine algae and higher plants, *J. Sea Res.*,
759 43(3–4), 183–197, doi:10.1016/S1385-1101(00)00030-7, 2000.
- 760 Stefels, J., and Van Boekel, W. H. M.: Production of DMS from dissolved DMSP in axenic cultures of the marine
761 phytoplankton species *Phaeocystis* sp., *Mar. Ecol. Prog. Ser.*, 97(1), 11–18, doi:10.3354/meps097011, 1993.
- 762 Stefels, J., Steinke, M., Turner, S., Malin, G., and Belviso, S.: Environmental constraints on the production and removal of the
763 climatically active gas dimethylsulphide (DMS) and implications for ecosystem modelling, *Biogeochemistry*, 83(1–3), 245–
764 275, doi:10.1007/s10533-007-9091-5, 2007.
- 765 Steinke, M., Malin, G., Archer, S. D., Burkill, P. H. and Liss, P. S.: DMS production in a coccolithophorid bloom: Evidence
766 for the importance of dinoflagellate DMSP lyases, *Aquat. Microb. Ecol.*, 26(3), 259–270, doi:10.3354/ame026259, 2002.
- 767 Stillman, J. H. and Paganini, A. W.: Biochemical adaptation to ocean acidification, *J. Exp. Biol.*, 218(12), 1946–1955,
768 doi:10.1242/jeb.115584, 2015.
- 769 Sunda, W., Kieber, D. J., Kiene, R. P., and Huntsman, S.: An antioxidant function for DMSP and DMS in marine algae, *Nature*,
770 418(6895), 317–320, 2002.



- 771 Toole, D. A., and Siegel, D. A.: Light-driven cycling of dimethylsulfide (DMS) in the Sargasso Sea: closing the loop, *Geophys.*
772 *Res. Lett.*, 31(9), 1–4, doi:10.1029/2004GL019581, 2004.
- 773 Toole, D. A., Slezak, D., Kiene, R. P., Kieber, D. J., and Siegel, D. A.: Effects of solar radiation on dimethylsulfide cycling in
774 the western Atlantic Ocean, *Deep. Res. Part I Oceanogr. Res. Pap.*, 53(1), 136–153, doi:10.1016/j.dsr.2005.09.003, 2006.
- 775 Toole, D. A., Siegel, D. A. and Doney, S. C.: A light-driven, one-dimensional dimethylsulfide biogeochemical cycling model
776 for the Sargasso Sea, *J. Geophys. Res. Biogeosciences*, 113(2), 1–20, doi:10.1029/2007JG000426, 2008.
- 777 Vallina, S. M., Simó, R., Anderson, T. R., Gabric, A., Cropp, R., and Pacheco, J. M.: A dynamic model of oceanic sulfur
778 (DMOS) applied to the Sargasso Sea: Simulating the dimethylsulfide (DMS) summer paradox, *J. Geophys. Res.*
779 *Biogeosciences*, 113(1), doi:10.1029/2007JG000415, 2008.
- 780 Vila, M., Simó, R., Kiene, R. P., Pinhassi, J., González, J. M., Moran, M. A., and Pedrós-Alió, C.: Use of microautoradiography
781 combined with fluorescence in situ hybridization to determine dimethylsulfoniopropionate incorporation by marine
782 bacterioplankton taxa, *Appl. Environ. Microbiol.*, 70, 4648–4657, <https://doi.org/10.1128/AEM.70.8.4648-4657.2004>, 2004.
- 783 Vila-Costa, M., Simó, R., Harada, H., Gasol, J. M., Slezak, D., and Kiene, R. P.: Dimethylsulfoniopropionate Uptake by
784 Marine Phytoplankton, *Science*, 314, 652–654, 2006a.
- 785 Vila-Costa, M., Del Valle, D. A., González, J. M., Slezak, D., Kiene, R. P., Sánchez, O., and Simó, R.: Phylogenetic
786 identification and metabolism of marine dimethylsulfide consuming bacteria, *Environ. Microbiol.*, 8, 2189–2200,
787 <https://doi.org/10.1111/j.1462-2920.2006.01102.x>, 2006b.
- 788 Vila-Costa, M., Pinhassi, J., Alonso, C., Pernthaler, J., and Simó, R.: An annual cycle of dimethylsulfoniopropionate sulfur
789 and leucine assimilating bacterioplankton in the coastal NW Mediterranean, *Environ. Microbiol.*, 9, 2451–2463,
790 <https://doi.org/10.1111/j.1462-2920.2007.01363.x>, 2007.
- 791 Vogt, M., Steinke, M., Turner, S., Paulino, a., Meyerhöfer, M., Riebesell, U., Le Quéré, C. and Liss, P.: Dynamics of
792 dimethylsulphoniopropionate and dimethylsulphide under different CO₂ concentrations during a mesocosm experiment,
793 *Biogeosciences*, 5(2), 407–419, doi:10.5194/bg-5-407-2008, 2008.
- 794 Webb, A., Malin, G., Hopkins, F., Ho, K. L., Riebesell, U., Schulz, K., Larsen, A., and Liss, P.: Ocean acidification has
795 different effects on the production of DMS and DMSP measured in cultures of *Emiliania huxleyi* and a mesocosm study: a
796 comparison of laboratory monocultures and community interactions, *Environ. Chem.*, 13(2), 314–329, doi:/10.1071/EN14268,
797 2015.
- 798 Webb, A. L., Leedham-Elvidge, E., Hughes, C., Hopkins, F. E., Malin, G., Bach, L. T., Schulz, K., Crawford, K., Brussaard,
799 C. P. D., Stühr, A., Riebesell, U., and Liss, P. S.: Effect of ocean acidification and elevated *f*CO₂ on trace gas production by a
800 Baltic Sea summer phytoplankton community, *Biogeosciences*, 13(15), 4595–4613, doi:10.5194/bg-13-4595-2016, 2016.
- 801 Wolfe, G. V., and Steinke, M.: Grazing-activated production of dimethyl sulfide (DMS) by two clones of *Emiliania huxleyi*,
802 *Limnol. Oceanogr.*, 41(6), 1151–1160, doi:10.4319/lo.1996.41.6.1151, 1996.
- 803 Woodhouse, M. T., Mann, G. W., Carslaw, K. S., and Boucher, O.: Sensitivity of cloud condensation nuclei to regional changes
804 in dimethyl-sulphide emissions, *Atmos. Chem. Phys.*, 13(5), 2723–2733, doi:10.5194/acp-13-2723-2013, 2013.



805 Yoch, D. C.: Dimethylsulfoniopropionate: Its sources, role in the marine food web, and biological degradation to
806 dimethylsulfide, *Appl. Environ. Microbiol.*, 68(12), 5804–5815, doi:10.1128/AEM.68.12.5804-5815.2002, 2002.
807



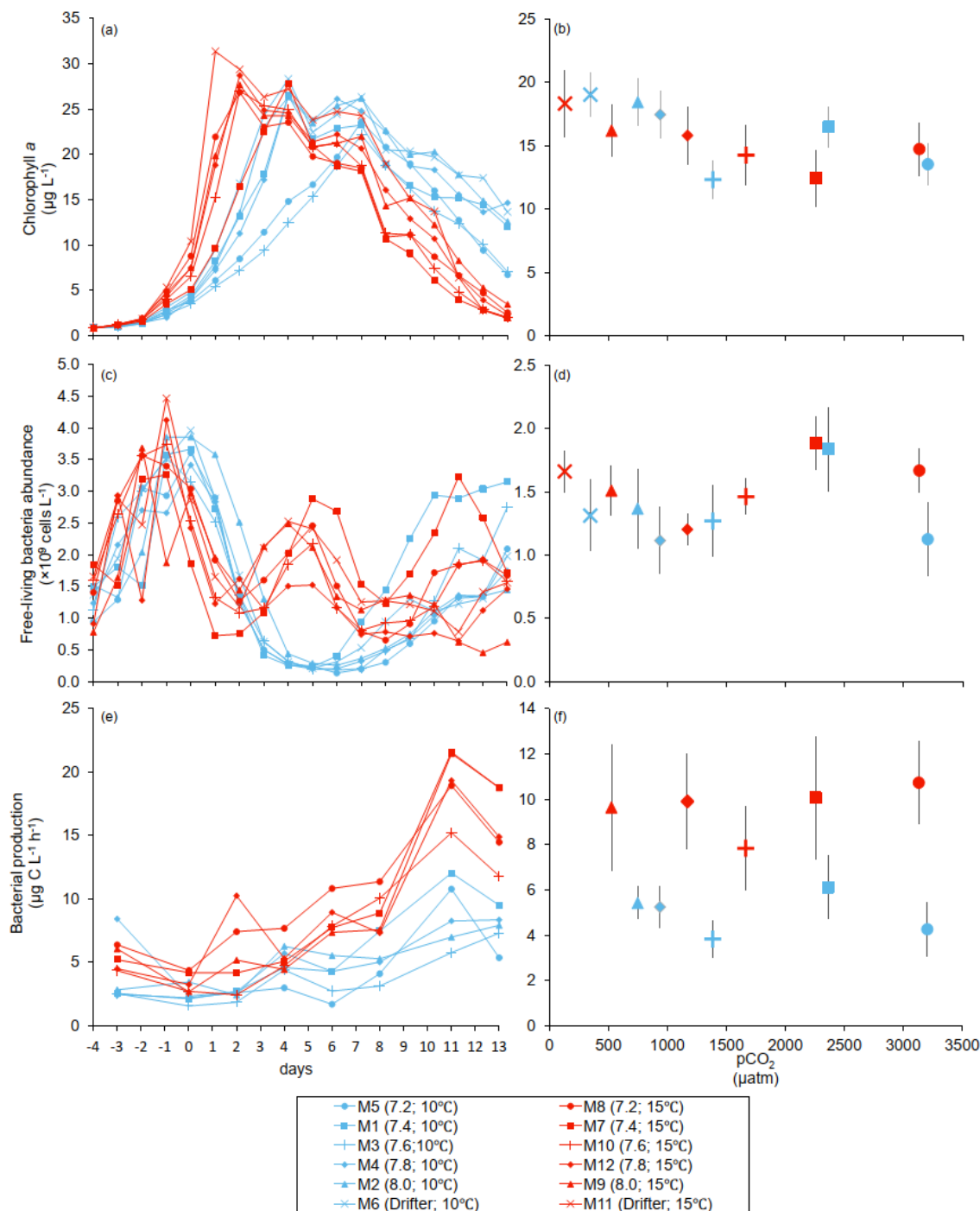
808

809

810

Figure 1. Temporal variations over the course of the experiment for: (a) temperature, (b) pH_T, (c) pCO₂. For symbol attribution to treatments, see legend. Adapted from B nard et al. (2018).

811



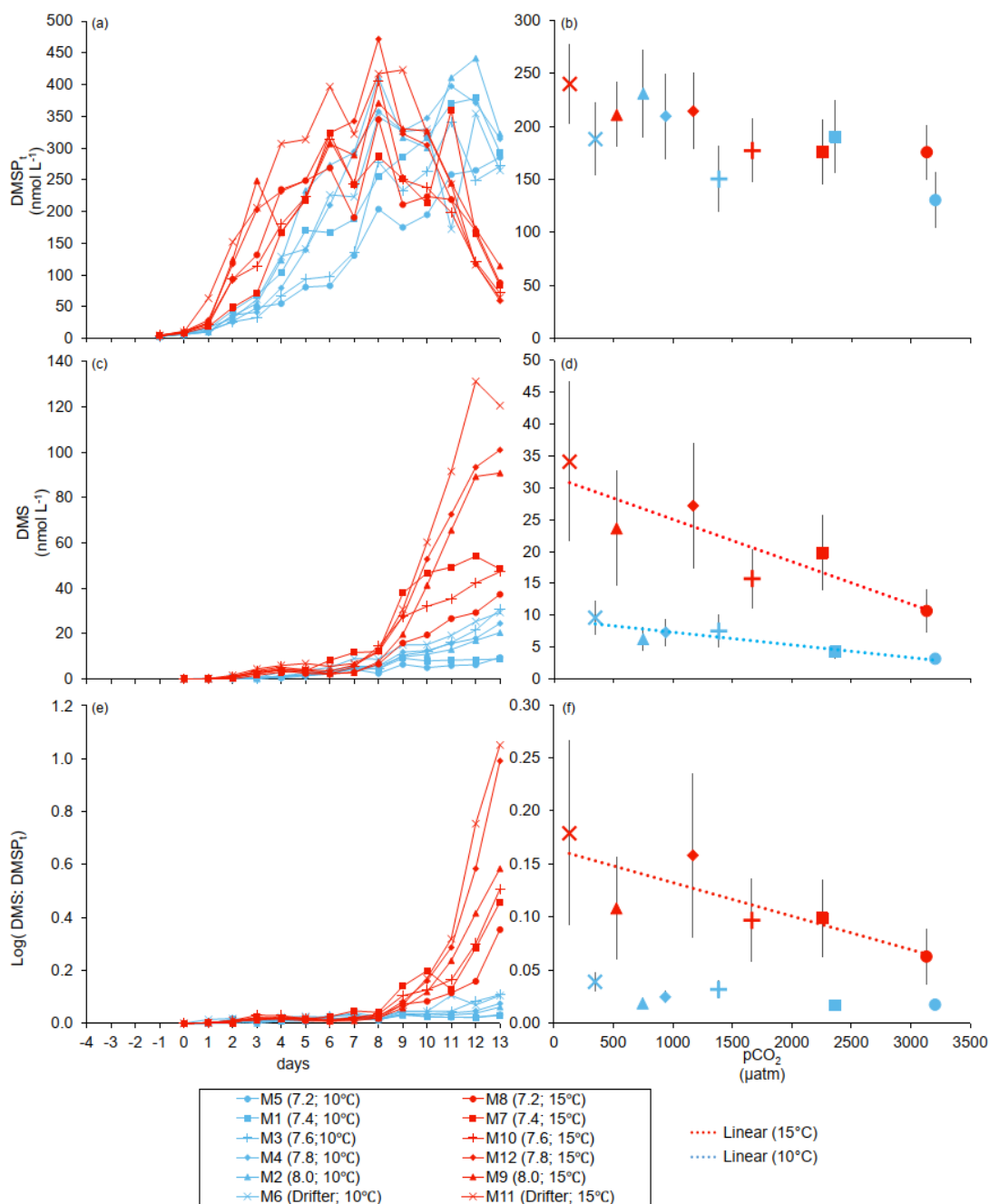
812

813

814

815

Figure 2. Temporal variations, and averages over the course of the experiment (day 0 to day 13) for: (a–b) chlorophyll *a* (adapted from B nard et al., 2018), (c–d) free-living bacteria abundance, (e–f) bacterial production. For symbol attribution to treatments, see legend.

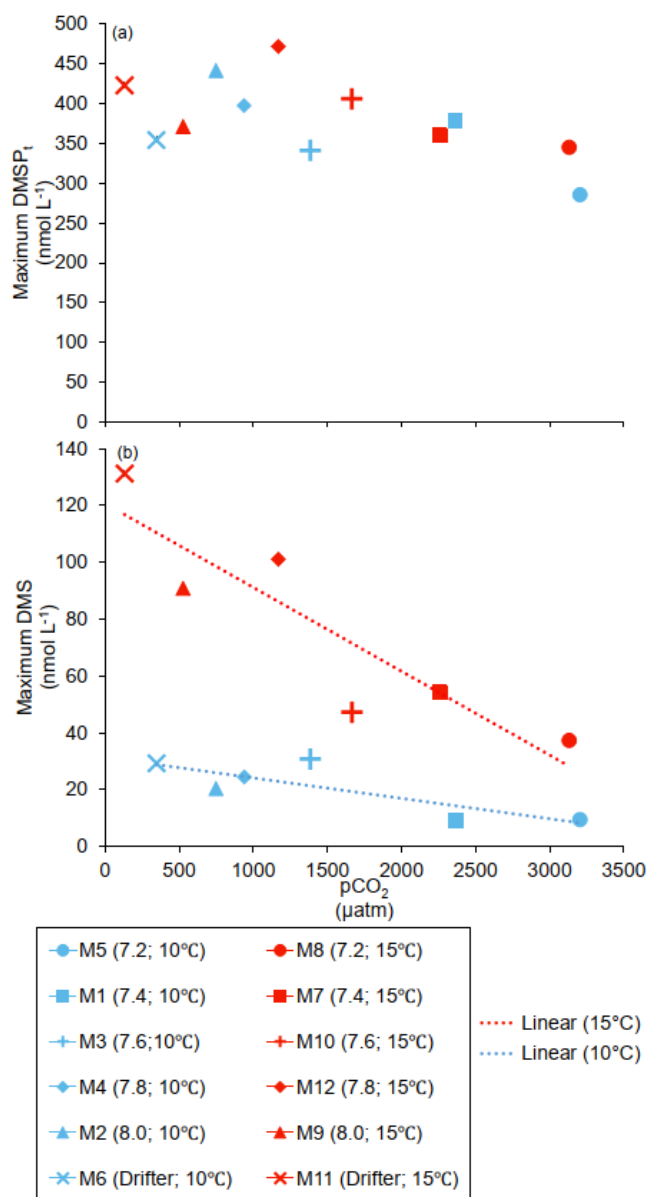


816

817

818

Figure 3. Temporal variations, and averages over the course of the experiment (day 0 to day 13) for: (a–b) DMSP_t, (c–d) DMS, (e–f) the natural logarithm of the DMS:DMSP_t ratio. For symbol attribution to treatments, see legend.

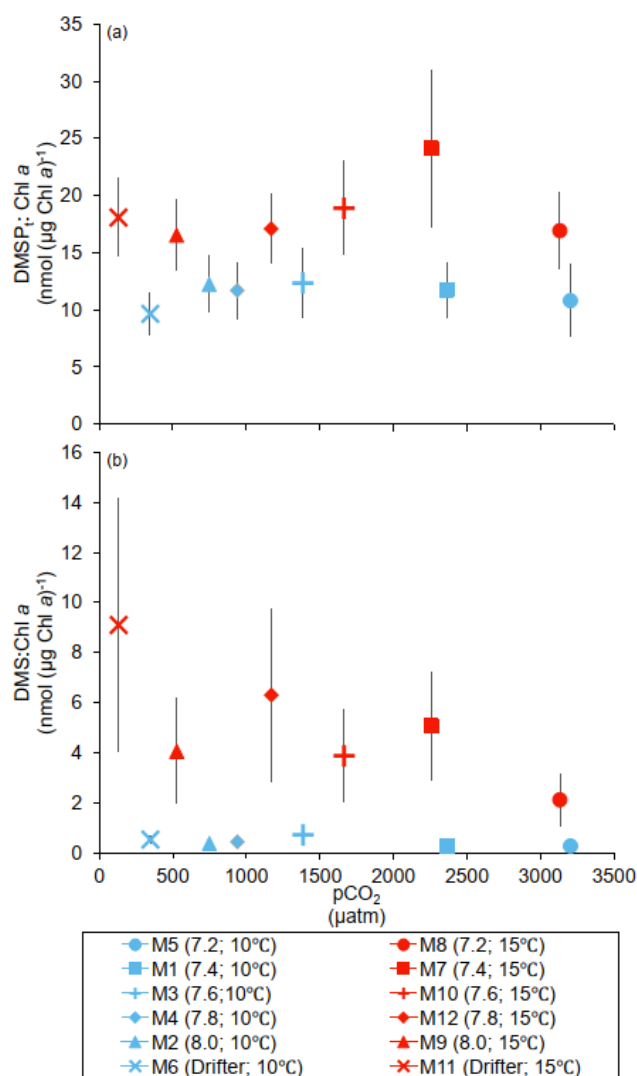


819

820

821

Figure 4. (a) Maximum DMSP_i concentrations, (b) maximum DMS concentrations reached over the full course of the experiment (day 0 to day 13). For symbol attribution to treatments, see legend



822

823

824

Figure 5. Averages over the course of the experiment (day 0 to day 13) for: (a) DMSP:Chl *a* ratio, (b) DMS:Chl *a* ratio. For symbol attribution to treatments, see legend.



825 **Table 1. Results of the generalized least squares models (glS) tests for the effects of temperature, pCO₂, and their interaction over**
 826 **the duration of the experiment (day 0 to day 13). Separate analyses with pCO₂ as a continuous factor were performed when**
 827 **temperature had a significant effect. Averages of bacterial abundance and production, DMSP_t, DMS, Chl *a*-normalized DMSP_t and**
 828 **DMS concentrations, and DMS:DMSP_t ratios are presented. Natural logarithm transformation is indicated when necessary.**
 829 **Significant results are in bold. *p<0.05, **p<0.01, ***p<0.001.**

830

Response Variable	Factor	df	t-value	p-value
Free-living bacterial abundance ($\times 10^9$ cells L ⁻¹)	Temperature	8	0.635	0.543
	pCO ₂	8	-0.083	0.936
	pCO ₂ x Temperature	8	0.221	0.830
Bacterial production ($\mu\text{g C L}^{-1} \text{ d}^{-1}$)	Temperature	6	2.454	0.050*
	pCO ₂ (10°C)	3	-0.272	0.803
	pCO ₂ (15°C)	3	0.746	0.510
DMSP _t (nmol L ⁻¹)	Temperature	8	0.509	0.625
	pCO ₂	8	-0.767	0.465
	pCO ₂ x Temperature	8	0.134	0.897
DMS (nmol L ⁻¹)	Temperature	8	6.822	<0.001***
	pCO ₂ (10°C)	4	-4.483	0.011*
	pCO ₂ (15°C)	4	-3.799	0.019*
DMSP _t :Chl <i>a</i> ratio (nmol ($\mu\text{g Chl } a$) ⁻¹)	Temperature	8	2.627	0.030*
	pCO ₂	8	0.123	0.908
	pCO ₂ x Temperature	8	0.621	0.568
DMS:Chl <i>a</i> ratio (nmol ($\mu\text{g Chl } a$) ⁻¹)	Temperature	8	5.225	<0.001***
	pCO ₂ (10°C)	4	-1.373	0.242
	pCO ₂ (15°C)	4	-2.227	0.090
Log(DMS:DMSP _t)	Temperature	8	5.131	<0.001***
	pCO ₂ (10°C)	4	-1.844	0.139
	pCO ₂ (15°C)	4	-3.138	0.035*

831

832



833 **Table 2. Results of the generalized least squares models (gls) tests for the effects of temperature, pCO₂, and their interaction on the**
 834 **maximum values of the parameters measured during the experiment. Separate analyses with pCO₂ as a continuous factor were**
 835 **performed when temperature had a significant effect. Maxima of DMSP_t, and DMS concentrations are presented. Significant results**
 836 **are in bold. *p<0.05, **p<0.01, ***p<0.001.**

837

Response Variable	Factor	df	t-value	p-value
DMSP _t (nmol L ⁻¹)	Temperature	8	0.384	0.711
	pCO ₂	8	-0.713	0.496
	pCO ₂ x Temperature	8	0.300	0.772
DMS (nmol L ⁻¹)	Temperature	8	6.403	<0.001***
	pCO ₂ (10°C)	4	-2.868	0.046*
	pCO ₂ (15°C)	4	-4.061	0.015*

838